

Sustainflatable: Harvesting, Storing and Utilizing Ambient Energy for Pneumatic Morphing Interfaces

Qiuyu Lu Carnegie Mellon University Pittsburgh, PA, USA qiuyul@cs.cmu.edu

Yuran Ding Carnegie Mellon University Pittsburgh, PA, USA yurand@andrew.cmu.edu Tianyu Yu Tsinghua University Beijing, China yty21@mails.tsinghua.edu.cn

> Haipeng Mi Tsinghua University Beijing, China mhp@tsinghua.edu.cn

Semina Yi Carnegie Mellon University Pittsburgh, PA, USA seminay@andrew.cmu.edu

Lining Yao Carnegie Mellon University Pittsburgh, PA, USA liningy@cs.cmu.edu



Figure 1: An example Sustainflatable system which can performs self-regulating plant insulation. The wind energy is harvest through a wind pump. The thermal valves incorporated in the system can sense the ambient temperature and adjust the inflation of the windbreaker accordingly. During warm weather, the windbreaker remains deflated (a). In contrast, during cold and windy weather, the system utilizes the collected energy to inflate the windbreaker and provide insulation to the plants (b).

ABSTRACT

While the majority of pneumatic interfaces are powered and controlled by traditional electric pumps and valves, alternative sustainable energy-harnessing technology has been attracting attention. This paper presents a novel solution to this challenge with the development of the Sustainflatable system, a self-sustaining pneumatic system that can harvest renewable energy sources such as wind, water flow, moisture, and sunlight, convert the energy into compressed air, and store it for later use in a programmable and intelligent way. The system is completely electronic-free, incorporating customized energy harvesting pumps, storage units with variable volume-pressure characteristics, and tailored valves that operate autonomously. Additionally, the paper provides a design tool to guide the development of the system and includes several environmental applications to showcase its capabilities.



This work is licensed under a Creative Commons Attribution-NonCommercial-ShareAlike International 4.0 License.

UIST '23, October 29−November 01, 2023, San Francisco, CA, USA © 2023 Copyright held by the owner/author(s). ACM ISBN 979-8-4007-0132-0/23/10. https://doi.org/10.1145/3586183.3606721

KEYWORDS

pneumatic interface, energy harvesting, energy harnessing, shape-changing interface

ACM Reference Format:

Qiuyu Lu, Tianyu Yu, Semina Yi, Yuran Ding, Haipeng Mi, and Lining Yao. 2023. Sustainflatable: Harvesting, Storing and Utilizing Ambient Energy for Pneumatic Morphing Interfaces. In *The 36th Annual ACM Symposium on User Interface Software and Technology (UIST '23), October 29–November 01, 2023, San Francisco, CA, USA*. ACM, New York, NY, USA, 20 pages. https://doi.org/10.1145/3586183.3606721

1 INTRODUCTION

Renewable energy sources have been utilized by humans since ancient times, as evidenced by the use of windmills [26] and waterwheels [67]. However, with the rise of the industrial revolution, the majority of our energy now comes from non-renewable fossil fuels such as oil, natural gas, and coal [28]. This dependence on non-renewable energy sources has resulted in environmental damage, energy crises, and climate change [21, 57].

To mitigate these problems, efforts have been made to increase the proportion of clean and renewable energy sources such as hydro, wind, and solar power [64]. Related to HCI, some researchers have focused on developing technologies for harvesting renewable energy to power wearable devices and interactive systems [10, 32, 42, 47, 82, 91]. While most of these technologies convert the harvested energy into electricity for storage and later use, recent work in the robotics field has demonstrated the feasibility of alternative pneumatic-energy-generating systems that can be more efficient, concise, and environmentally friendly [55, 56, 74].

Despite the growing interest in pneumatic interfaces in the human-computer interaction (HCI) field [20, 23, 24, 37, 39, 44, 51, 58, 70, 76, 79, 80, 86, 92–94], most current pneumatic interfaces are still powered by electronic pumps and valves, which limits their application in broader contexts. To address this limitation, this paper investigates how to harvest various ambient renewable energy sources, convert them to compressed air, and store the compressed air for later actuating utilization in a pre-programmed way.

We hope this research can promote the development of sustainable pneumatic interfaces that can operate autonomously in an ambient environment and potentially be used in a wide range of applications. The core contributions of this work are as follows:

- A three-phase ambient energy harnessing strategy for the pneumatic interface:
 - Harvesting: non-electric pumps that can harvest a variety of ambient energy sources and leverage this energy to compress air:
 - Storage: storage units with distinct volume-pressure characteristics to store the compressed air for different demands;
 - Utilization: non-electric valves that are triggered by environmental factors with tunable thresholds to manage the compressed air for actuation autonomously;
- A corresponding design tool that:
 - guides users through the process of designing the system;
- provides estimation of working results for quick iterations;
- exports material list and fabrication instructions to facilitate prototyping.
- Functional performance evaluation of the Susbtainflatable system
- Several application examples that demonstrate the capability of the Susbtainflatable system.

2 RELATED WORK

2.1 Pneumatic Interface

Over the past few decades, significant progress has been made in developing materials and methods for fabricating pneumatic (and hydraulic) tangible interfaces [31, 48], enhancing their shape-changing and display capabilities, and improving their actuation structures [19, 38–40, 44, 49, 58, 70, 76, 92–95]. There have also been investigations into using these interfaces for sensing technologies [24, 44, 79, 86] and exploring the use of more compact electronic pumps for actuation [20, 51]. Additionally, the technical advancements of these interfaces have led to various studies exploring application contexts and evaluating user experiences, with a particular focus on exploring diverse haptic feedback experiences [13, 23, 36, 37, 80, 81]. Recently, several works have started to explore unconventional mechanical computing technologies [14, 41, 71]. These technologies offer an alternative method for controlling such interfaces, which can supplement or even replace electronic

boards. Unlike traditional electronic control systems, these unconventional control systems operate rely on fluidic current instead of electric current.

However, most of these systems still require an electronic pump to provide compressed air or pressurized liquid. To address this limitation, researchers have investigated alternative actuation methods. For example, gas-producing chemical reactions have been adopted. But they require manual refueling of chemicals [90], and some of the reactions can be difficult to stop, resulting in a one-time use only [89]. Low boiling-point liquids (LBLs) have also been investigated for their potential to leverage ambient thermal energy for actuation [39, 50]. However, LBL-based inflatables lack controllability and on-demand responses, as they deform or reverse directly in response to changes in environment temperature in this case. Slightly off-topic from the HCI field, some researchers have started exploring the possibility of using human motion to generate energy for powering pneumatic assistive garments [55, 56, 74].

Overall, the current body of research in pneumatic interfaces and robotics lacks a further exploration of how to harvest and convert various ambient renewable energy sources into compressed air. Furthermore, existing research doesn't sufficiently explore the intelligent and programmable storage and utilization of this compressed air, particularly in a non-electronic manner. Identifying and addressing these gaps in research propels us towards not only creating more sustainable and efficient pneumatic power solutions but also advancing towards a greener approach in renewable energy usage.

2.2 Sustainablility in HCI

Sustainability is an increasingly important topic in HCI, given the significant impact of technology on the environment and social equity [46]. HCI researchers explored ways to promote sustainability

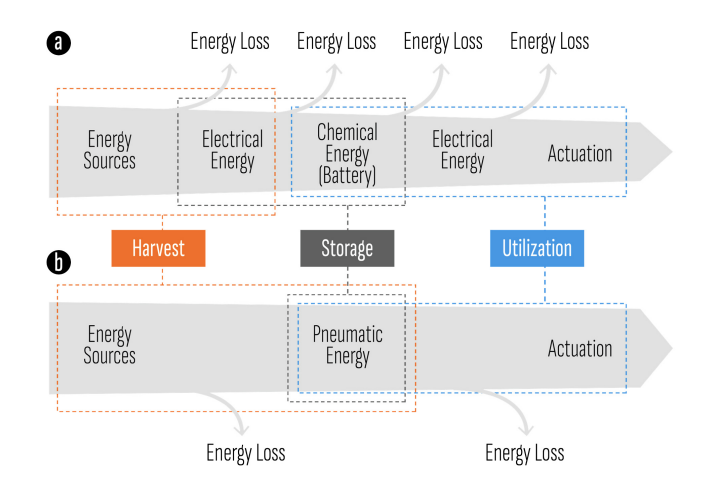


Figure 2: A comparison between an electrical energy generating system (a) and a pneumatic energy generating system (b) shows that the latter has the potential to be more energy-efficient, more concise, more cost-effective construction, and reduce the use of hazardous materials like heavy metals. Revised based on the figure from [73].

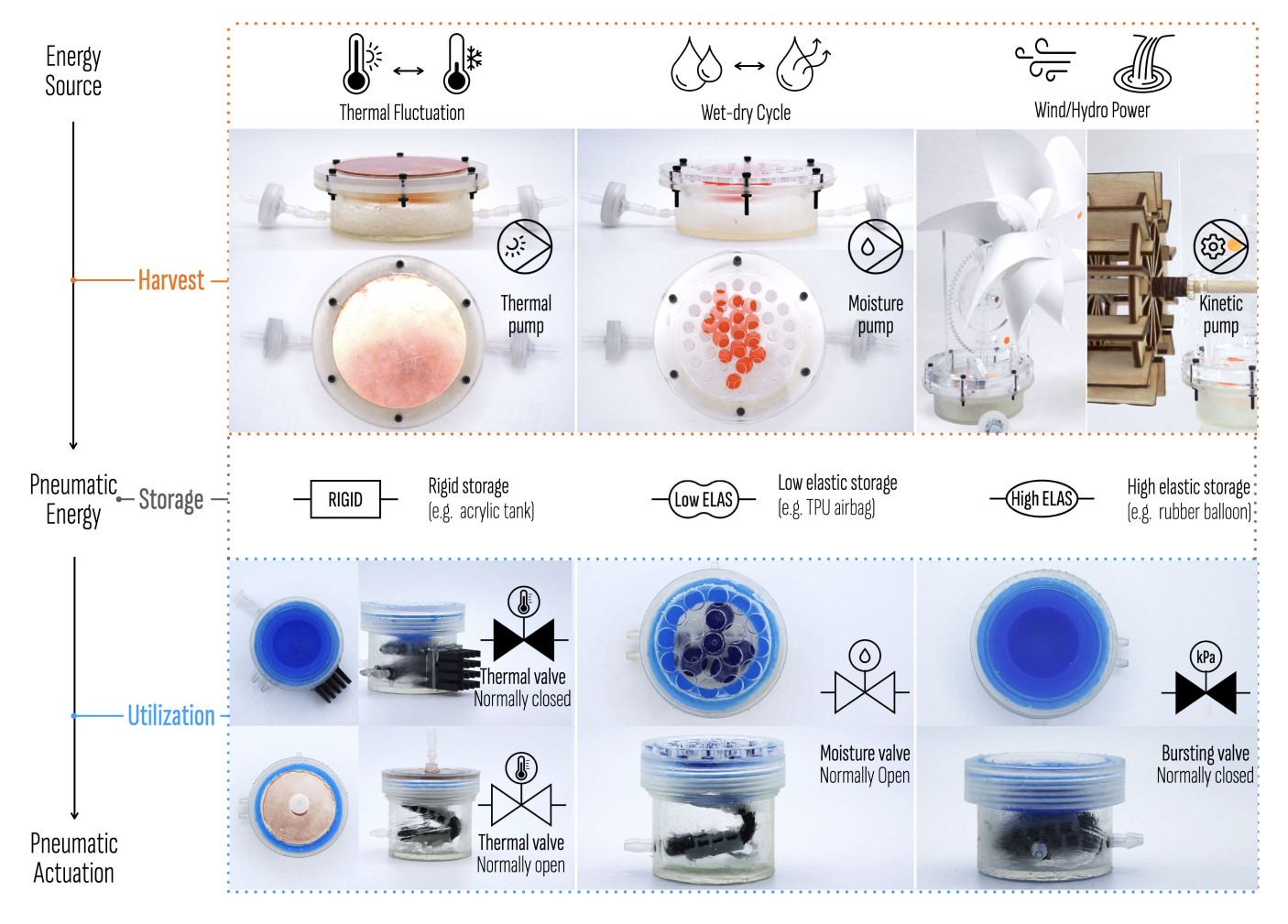


Figure 3: The three-phase energy harnessing solution provided by Sustainflatabe.

in interactive devices, such as degrading, recycling, and harnessing energy in a sustainable manner. One trend is using degradable material for prototyping interactive devices, such as heating plastic wireless interfaces [75], soft interactive biodegradable devices [34], flexible vinyl fabric-like alganyl [4], electronic devices with mycelium [84] and wood veneer-based self-drilling interfaces [42]. These devices offer easy breakdown and superior degradability, leading to reduced contamination and overall sustainability.

At the same time, another significant effort in HCI research is in recycling. Projects like Digital Mechanical Metamaterials [29], Airlogic [71], and Fluidic Computation Kit [41] have facilitated easy recycling by creating electronic-free interactive devices that may be fully recycled based on their materials, without complex disassembly. Researchers have also explored opportunities for reusing scrap materials [18, 35, 88] and upcycling waste materials [9] to reduce waste and promote sustainability.

Lastly, various technologies are investigating harnessing energy for powering interactive devices. This approach can enable sustainable and self-powered devices that do not require external power sources [1, 2, 7, 15, 47, 82, 85]. While most of these systems focus on converting human kinetic energy to electric energy for electronic devices, we focus on developing non-electronic technologies that harness a broader range of renewable energy sources beyond human motion to generate pneumatic power. This substantially widens the scope of renewable energy sources that can be harnessed to power interfaces. Moreover, we have developed a design tool to foster engagement and adoption from both researchers and everyday users in creating and utilizing such ambient renewable energy powered systems.

2.3 Energy Harvesting Technologies

To power portable or wearable electric systems, energy can be harvested from sources such as solar, biomechanical, and biochemical through mechanisms like photovoltaics, piezoelectric, triboelectric, or electromagnetic conversion [10, 32, 91]. However, each energy transformation step in these systems results in energy loss, as shown in Fig. 2.a [73]. For instance, in an electrically powered pneumatic system, a significant amount of energy is lost in the step of powering the pump to generate compressed air for actuation. Specifically, 80%-90% of the energy is dissipated as heat [28].

When it comes to a pneumatic system, a more direct and nonelectric process can be adopted (Fig. 2.b). The energy only changes from the original source to pneumatic energy. Pneumatic energy can be easily stored and used without conversion, leading to improved energy efficiency, simpler and more cost-effective construction, and reduced use of hazardous materials such as heavy metals.

Following this non-electricity-involved strategy, researchers have developed pneumatic wearable assistive devices powered by compressed air generated by human-motion-induced energy, particularly from foot strike [55, 56, 74]. While in this paper, we further explored harvesting other energy sources, especially ambient energy sources that can allow the pneumatic system to work unattended and even outdoors, expanding its applicability.

Moreover, the current main approaches for utilizing compressed air still rely on manually or electrically operated valves. There are potential technologies that can be leveraged to improve this, including pressure-difference-operated pneumatic valves and computation [16, 41, 62, 65, 66, 71]. Additionally, in the microfluidic field, various micro valves triggered by temperature, humidity, radiation, etc., have been explored [25, 72, 87]. To complete the loop (Fig. 2.b) and enable a completely autonomous system, we developed a series of ambient environmental triggered non-electric "macro" valves, enabling the pneumatic system to work autonomously without the need for external power or human intervention.

3 SUSTAINFLATABLE OVERVIEW

To achieve the goal of harnessing ambient energy for a pneumatic interface, we propose a three-phase solution (Fig. 3). Firstly, we employ various non-electric pumps that can harvest a variety of ambient energy sources and leverage this energy to compress air. We then utilize storage units with distinct volume-pressure characteristic curves to store the compressed air. Finally, we incorporate various non-electric valves that are triggered by environmental factors with tunable thresholds to manage the compressed air.

3.1 Pumps for Energy Harvesting

In this section, we will present the design, mechanism, and evaluation of pumps designed for harvesting ambient thermal, moisture, and kinetic energy.

3.1.1 Thermal Pump. A thermal pump can leverage temperature fluctuations to compress air. The structure of a thermal pump is shown in Fig. 4.a, b. The laser-cut acrylic lid contains a copper plate embedded in the middle and a bladder with a low-boiling-point liquid (LBL) attached to the bottom of the copper plate using a round thermal adhesive tape. The 3D printed body has two ports with check valves installed to ensure that air flows only in one direction, from the inlet to the outlet. The lid, sealing ring (Ecoflex 00-30), and body are held together with screws and nuts.

When the ambient temperature rises above the boiling point of the LBL liquid, the bladder expands and pushes the air out from the outlet (Fig. 4.c2). Conversely, when the ambient temperature drops below the boiling point, the bladder contracts, and the pump refills with air through the inlet (Fig. 4.c1).

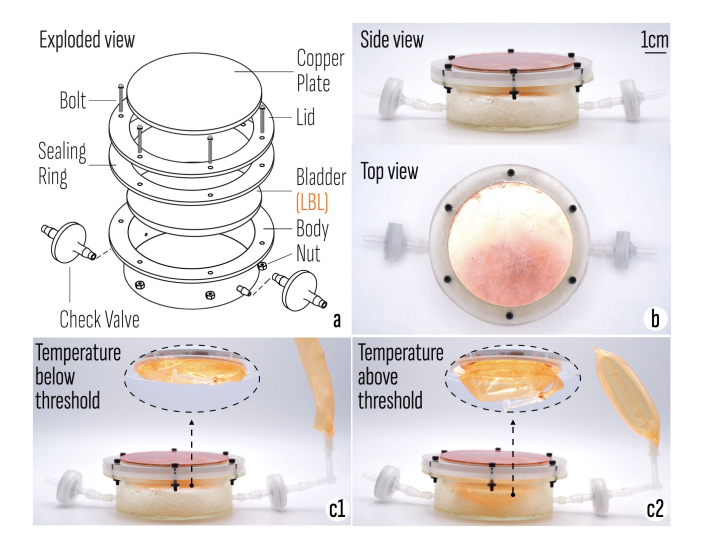


Figure 4: The thermal pump: a). The exploded view of the structure. LBL stands for Low Boiling Point Liquid which is pre-injected to the bladder before assembly. b). The side view and top view of the pump. c). The LBL bladder inside the pump performs cyclic deflation (c1) and inflation (c2) as the environment temperature fluctuates, gradually pumping air to the target airbag.

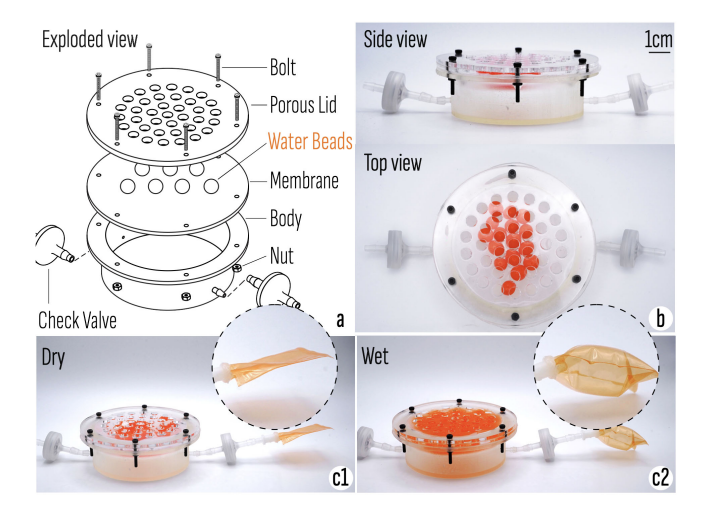


Figure 5: The moisture pump: a). The exploded view of the structure. b). The side view and top view of the pump. c). The water beads perform cyclic deswelling (c1) and swelling (c2) along with the wet-dry cycle, gradually pumping air to the target airbag.

In this paper, we demonstrate and experiment with Novec 7000 1 as our primary working medium for the thermal pump (and thermal valve), which has a boiling point of 34° C. However, it's worth noting that 3M offers a range of other Novec products with boiling points

 $^{^13}M$ Novec 7000 Engineered Fluid

ranging from 49° C to 128° C 2 , which can also be used. Furthermore, the thermal pump requires a very small amount of LBL, typically less than 2 mL, which is sealed in the bladder for cyclic use and isolated from the atmosphere. Therefore, some flammable LBLs such as 1,2-Butadiene (boiling point 10.9° C) and acetaldehyde (boiling point 20.8° C) may also be used but need to be handled carefully during filling.

3.1.2 Moisture Pump. A moisture pump can utilize dry-wet cycles to compress air. The structure of a moisture pump is shown in Fig. 5.a, b. The pump consists of a porous lid that allows water to enter and evaporate. The body of the moisture pump is the same as that of the thermal pump. However, a thin elastic silicone membrane (Ecoflex 00-30) is clamped in the middle instead of a sealing ring. Off-the-shelf water beads are placed between the lid and the membrane. Its diameter can increase from ~ 6 mm to ~ 40 mm after swelling. When the pump gets wet, the water beads swell and push the air out from the outlet (Fig. 5.c2). Conversely, when the pump dries out, the water beads deswell, and the pump refills with air through the inlet (Fig. 5.c1)

the inlet (Fig. 5.c1). 3.1.3 Kinetic Pump. A kinetic pump can use mechanical energy such as wind power or hydro energy to compress air. The structure of two types of kinetic pump is shown in Fig. 6.a. It has an identical body to the moisture pump and uses the same membrane. However, the lid of the kinetic pump has integrated mechanisms that are powered by either the wind or flowing water. These mechanisms convert the rotational motion of the windwheel (Fig. 6.b) or waterwheel (Fig. 6.c) to linear reciprocating motion of the piston. As the slider moves down, it presses the membrane and pushes the compressed air out through the outlet (Fig. 6.d1). Conversely, when the slider moves up, the membrane is pulled up, and the pump refills with air through the inlet (Fig. 6.d2).

3.1.4 Performance Evaluation and Comparison of Pumps. The pump performance evaluation results are presented in Fig. 7.

Thermal pump. The thermal pump had a low boiling liquid (LBL, Novec 7000) in the bladder and was equipped with a single port 60 mm × 60 mm square thermoplastic airbag to its outlet. The air pressure at the airbag port was monitored throughout the experiments (Fig. 7.a). To initiate the test, the thermal pump was kept at 20°C and placed upside down to enhance the heat conductivity of the bottom copper plate. For each testing cycle, the pump was placed at 40°C for 90 s and then back to a 20° for another 90 s. This cycle was repeated until the pressure reached its plateau (Fig. 7.c). Moreover, we also conducted an experiment more reflective of natural environmental temperature fluctuations, where each 24-hour cycle incorporated a gradual temperature shift: 0h/20°C -12h/40°C - 24h/20°C. Air pressure was documented at the end of each cycle. The general trend of pressure change was similar to that observed in Fig. 7.c, with the primary distinction being that the pressure peaked at 20 kPa during the 8th or 9th cycle in three repeat experiments, which took more cycles than the 180s cycle experiment. This can be attributed to the small, slow leak in the system.

As shown in the first row of Figure 7.b, the reference average pumping rate (Ref. R, ~ 0.24 mL/s) and the reference pumping volume each cycle (Ref. V, ~ 22 mL) were determined based on the

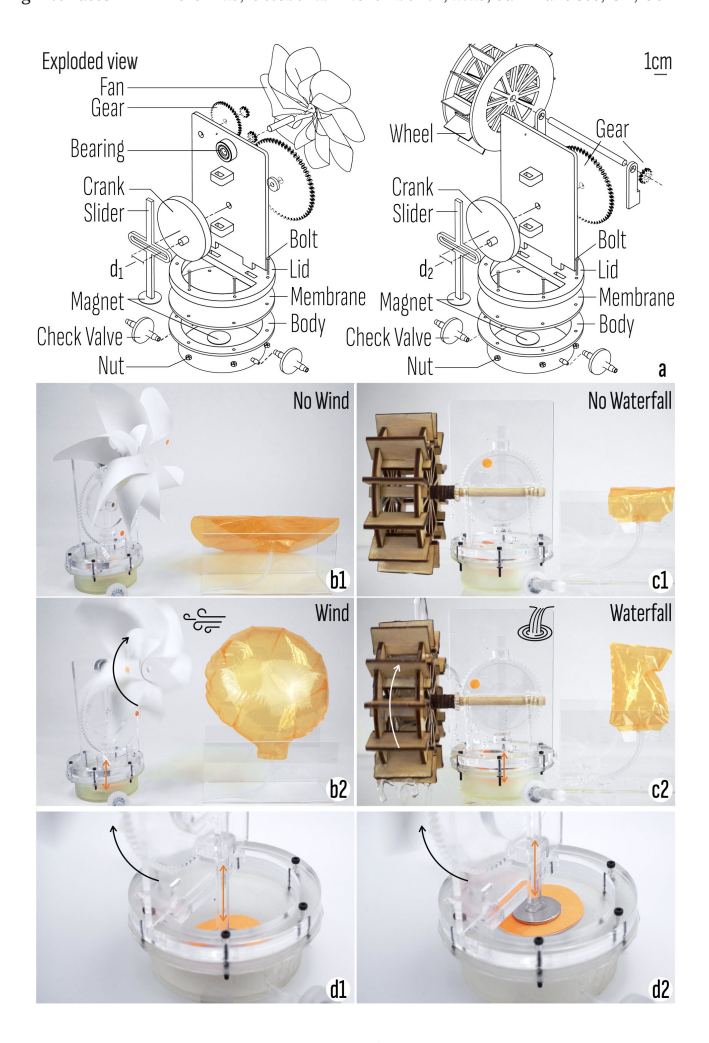


Figure 6: The kinetic pumps: a) The exploded view of the structure. The d2 is smaller than d1 to reduce the pressing distance of the slider, as the wood rod of the waterwheel is observed to have higher friction with the acrylic stand. b). The kinetic pump is powered by wind to generate compressed air. c). The kinetic pump is powered by a waterfall to generate compressed air. d), The piston is pushing the membrane down (d1) and pulling the membrane up (d2) periodically, pumping air to the target airbag.

first cycle at a temperature shift from 20 to 40°C before the pressure of the airbag was built up. To understand how the performance of the thermal pump changes with temperature ranges, as the Figure 7.c insert shows, the maximum pressure (Max. P) under different temperature fluctuation ranges was measured. While we observed that the Max. P for each pump remains relatively constant during repeated experiments under the same conditions, the number of cycles before reaching the maximum pressure may vary a little. This variability may be attributed to minor fluctuations in external factors such as wind or water flow, humidity level, etc.

Moisture pump. The experimental setup for the moisture pump was similar to that of the thermal pump, with the main difference

 $^{^2 \}mbox{Novec}$ Engineered Fluid comparison

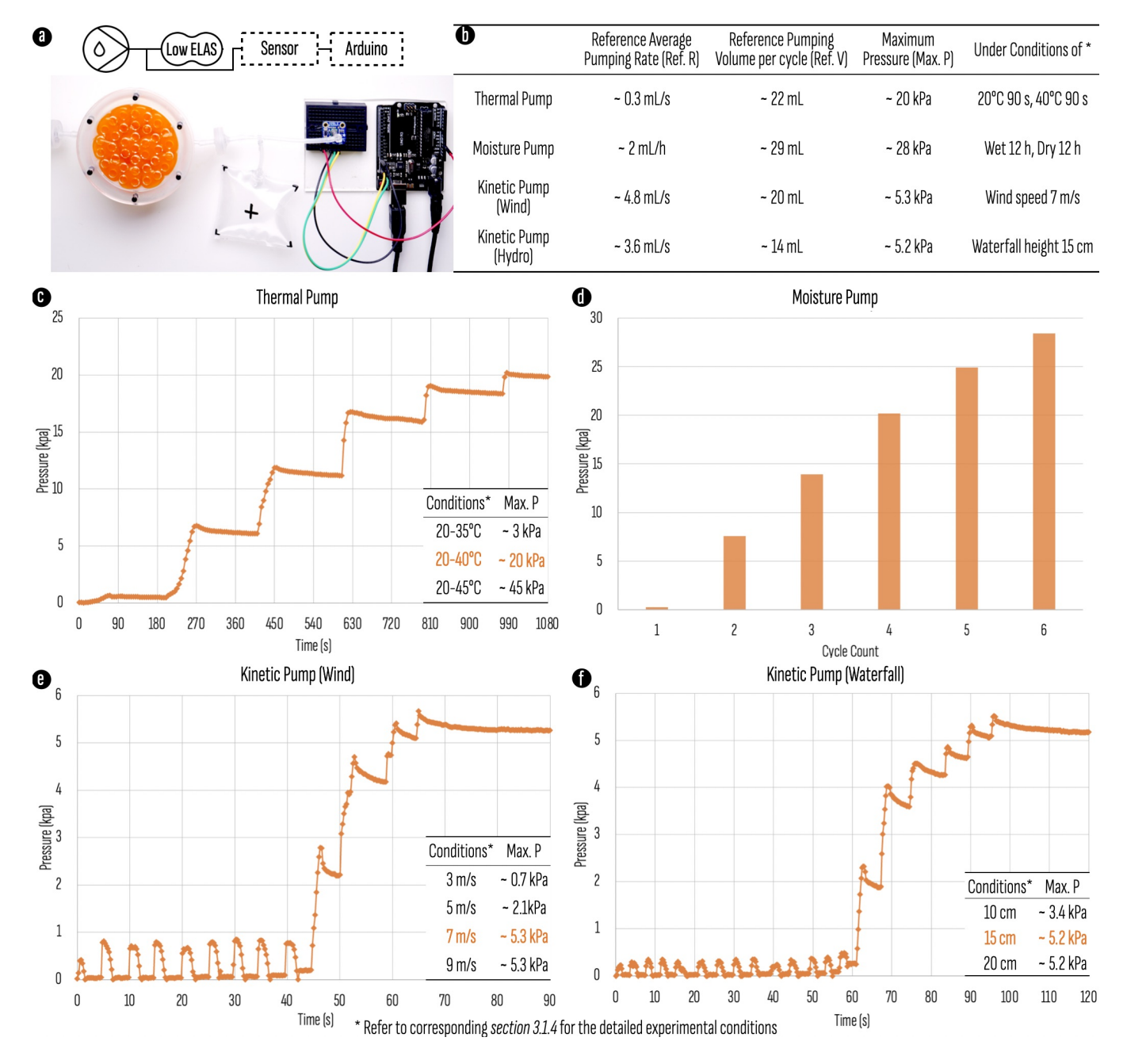


Figure 7: The performance evaluation results of the energy harvesting pumps. a). The air pressure measure setup, taking the moisture pump as an example. b). Summary table of the results. Sample size is 3 for each test. c-f). The time-pressure relationship of the thermal pump under the 90s-20°C-90s-40°C cycle (c), the moisture pump under the 12 h-wet-12 h-dry cycle (d), the kinetic pump under a $\sim 7\text{m/s}$ wind (e), the kinetic pump under a 15 cm high, 15 mm thick, 100 mL/s water flow.

being that the moisture pump was kept wet for 12 h at room temperature and then transferred to a 40 $^{\circ}$ C drying box for 12 h. This cycle was repeated until the water beads could no longer withstand the pressure and showed visible cracks. The Ref. R and Ref. V were determined based on the first wet-dry cycle (Fig. 7.b, d).

Kinetic pump. The kinetic pumps tested in this study both featured a single port 100 mm ×100 mm square thermoplastic airbag connected to their outlet. Fig. 7.e and f present the test results for the wind kinetic pump under moderate wind conditions (\sim 7m/s) and the water flow kinetic pump under a water flow with a height of 15 cm, a flow rate of \sim 100mL/s, and a diameter of \sim 15 mm. The

Ref. R and Ref. V reported in Figure 7.b were determined on the same conditions with the first several cycles before the pressure of the airbag built up. In addition, the maximum pressures were also measured for different wind speeds and waterfall heights (see inserts in Fig.7.e and f).

In summary, the thermal pump and moisture pump are capable of generating higher compressed air pressure of ~ 20 kPa or more under appropriate conditions, while the kinetic pump can reach a pressure of ~ 5 kPa. This limitation primarily arises from the deformation of the thin membrane edge of the kinetic pump, which tends to deform upwards when subjected to high pressures. In addition, according to Ref. R, kinetic pumps have the largest average pumping rates (Ref. R) among all pumps tested. The pumping rate of the thermal pump is mainly limited by the speed of ambient temperature fluctuation, while the moisture pump is limited by the speed of (de)hydration of the water beads in real-world applications.

3.2 Stimuli Responsive Valves for Energy Utilization

The valves utilized in this system primarily rely on the tube kinking and/or the bistable membrane phenomenon for their operation. Tube kinking occurs when a flexible tube is bent or compressed to a certain extent, causing it to fold or collapse in on itself and obstruct the flow path [43]. The bistable semi-spherical membrane is a structure capable of existing in two stable equilibrium states [6]. Changes in air pressure between the two sides of the membrane can force it to transition between states, and its geometric parameters can be tuned to adjust the threshold pressure [33, 77].

By combining these two mechanisms, Rothemund et. al proposed a pressure-difference-operated bistable valve [68], which has since been utilized in the development of many pneumatic soft robot technologies [61, 62, 65].

Pushing it further, we developed reconfigurable valves triggered by various environmental factors. Different lid, body, (bistable)

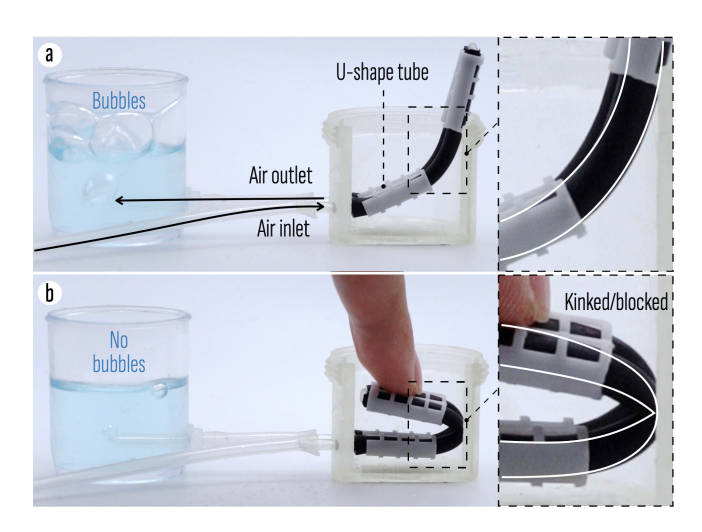


Figure 8: Demonstrating the tube-kinking phenomenon. The tube will kink and block the air flow when it is forced to fold (a to b).

membrane and working medium designs can be combined for various environmental factors, making the system more adaptable, versatile, and autonomous. The tubes are positioned horizontally and enhanced with exoskeletons, which allows for easier pressing and kinking (Fig. 8). These developments not only improve the functionality of the Sustainflatable system but also pave the way for more innovative applications in various conditions.

3.2.1 Bursting Valve. A bursting valve is designed to respond to changes in air pressure and either open or close accordingly. The bursting valve's structure is illustrated in Fig. 9.a, b and consists of a 3D printed body with male thread, a 3D printed hollow lid with female thread, a casted bistable membrane (Mold Star 30), and two rubber tubes accompanied with 3d printed exoskeletons and a u-connector. The body has a pair of inlet/outlet ports, and a third control port. The control port and the inlet can either share the same or different air source.

The bistable membrane enabled valve operates when the air pressure at the control port exceeds a certain threshold, causing the bistable membrane to snap upward and un-kink the tubes (Fig. 9.c). This results in the bi-bursting valve remaining open unless there is negative pressure in the control channel or external force applied to the membrane. A monostable membrane may be used to let the valve reset and close automatically when air pressure drops.

3.2.2 Thermal Valve. A thermal valve can respond to changes in ambient temperature. There are two types of thermal valves: normally closed (NC) and normally open (NO). The thermal valve also utilizes LBL as the working medium, similar to the thermal pump introduced earlier. By modifying the LBL material, the thermal valve can achieve various temperature thresholds. The NC thermal valve will open once the temperature goes beyond the threshold,

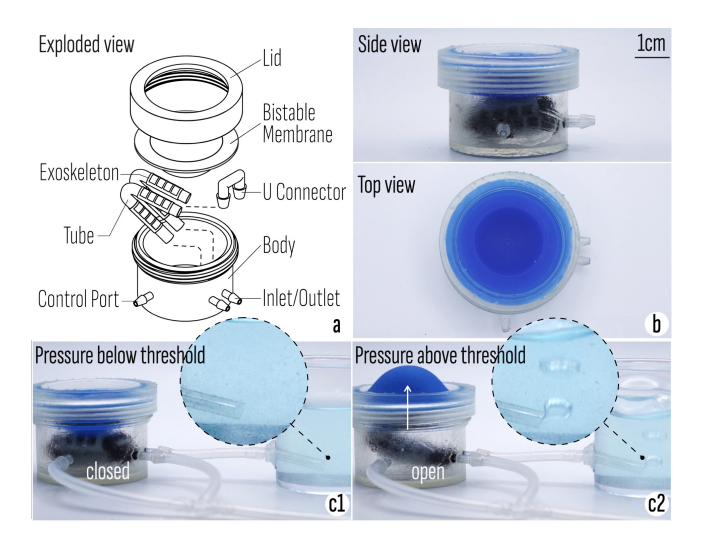


Figure 9: The bursting valve: a). The exploded view of the structure. b). The side view and top view. c). The valve remains closed when the air pressure is below the threshold (c1), and bursts to open when the air pressure is above the threshold (c2). The control port and the inlet are sharing the same air source in this figure.

while the NO thermal valve works in the opposite way. Both NC and NO thermal valves are reversible.

The structure of the thermal valves is shown in Fig. 10.a - d. Compared to the bursting valve, the NC thermal valve has a window on the body with a heat sink mounted, and the third port acts as a liquid filling port for LBL. When the LBL turns into gas due to a rise in temperature, the internal pressure will increase and force the membrane to deform upward, gradually unkinking the tubes and opening the valve (Fig. 10.e2). Then, when the LBL cools down and turns back into liquid, the negative internal pressure will pull the membrane back and kink the tubes (Fig. 10.e1). In the NC thermal valve, the filling port is sealed, creating an enclosed space with a very limited volume, which weakens the bistable performance of the membrane. However, the bistable behavior is not necessary for the NC thermal valve's operation. The valve will open/close before the membrane completely snaps through/back.

As for the NO thermal valve, it features a small copper-plateembedded lid for efficient heat conduction, and a top center port

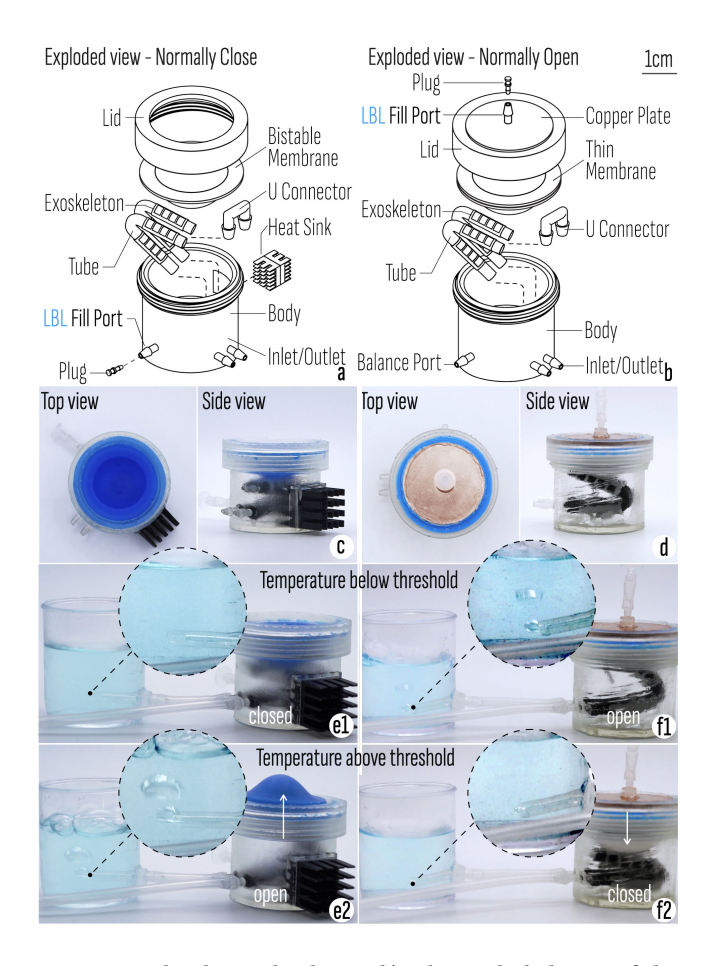


Figure 10: The thermal valves: a,b). The exploded view of the structure. c,d). The side view and top view. e). The normally closed thermal valve will open when the temperature is above the threshold. f). The normally open thermal valve will close when the temperature is above the threshold

for filling LBL. The balance port on the valve body is left open to maintain a constant atmospheric internal pressure. The membrane is mainly made of a low shore hardness silicone material (Ecoflex 00-30), which tends to wrinkle during lid screwing, causing air leaks. To reinforce the edge, a relatively rigid silicon ring (Mold Star 30) is casted and glued (using Sil-poxy) with the membrane. As the LBL turns into gas, the membrane inflates and kinks the tubes (Fig. 10.f2)., and when the LBL cools down and turns back into liquid, the membrane deflates, and the tubes automatically unkink (Fig. 10.f1).

Both types of thermal valves have a slightly taller body than the bursting valve to avoid interference between the bistable membrane and the heat sink in the NC thermal valve, and to ensure the tubes are completely unkinked in the NO thermal valve. Additionally, the NC thermal valve body has a padding slope on the bottom to ensure its tubes can be fully kinked when triggered.

3.2.3 Moisture Valve. A moisture valve can be triggered by the dry-wet cycle. Its structure is similar to that of a NO thermal valve and is illustrated in Fig. 11.a, b. However, instead of a copper plate embedded in the lid, a porous acrylic is used. The working medium in this valve are water beads, which will swell when wetted, pushing down the membrane to kink the tubes (Fig. 11.c1-c4). When the water beads dry out, they will deswell, allowing the membrane to recover and the tubes will unkink by themselves. For the same reason as the NO thermal valve, the moisture valve also has a relatively taller body.

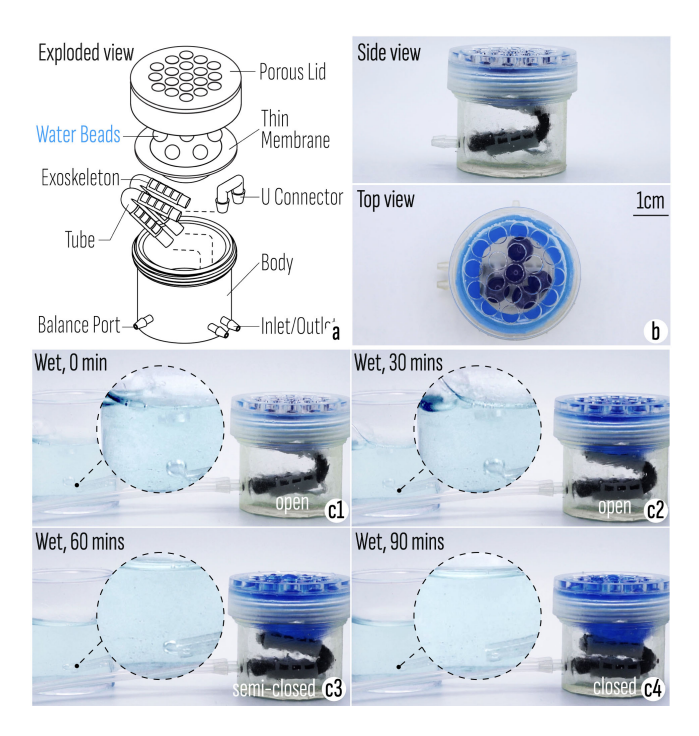


Figure 11: The moisture valve: a). The exploded view of the structure. b). The side view and top view. c). The valve gradually closes when it gets wet.

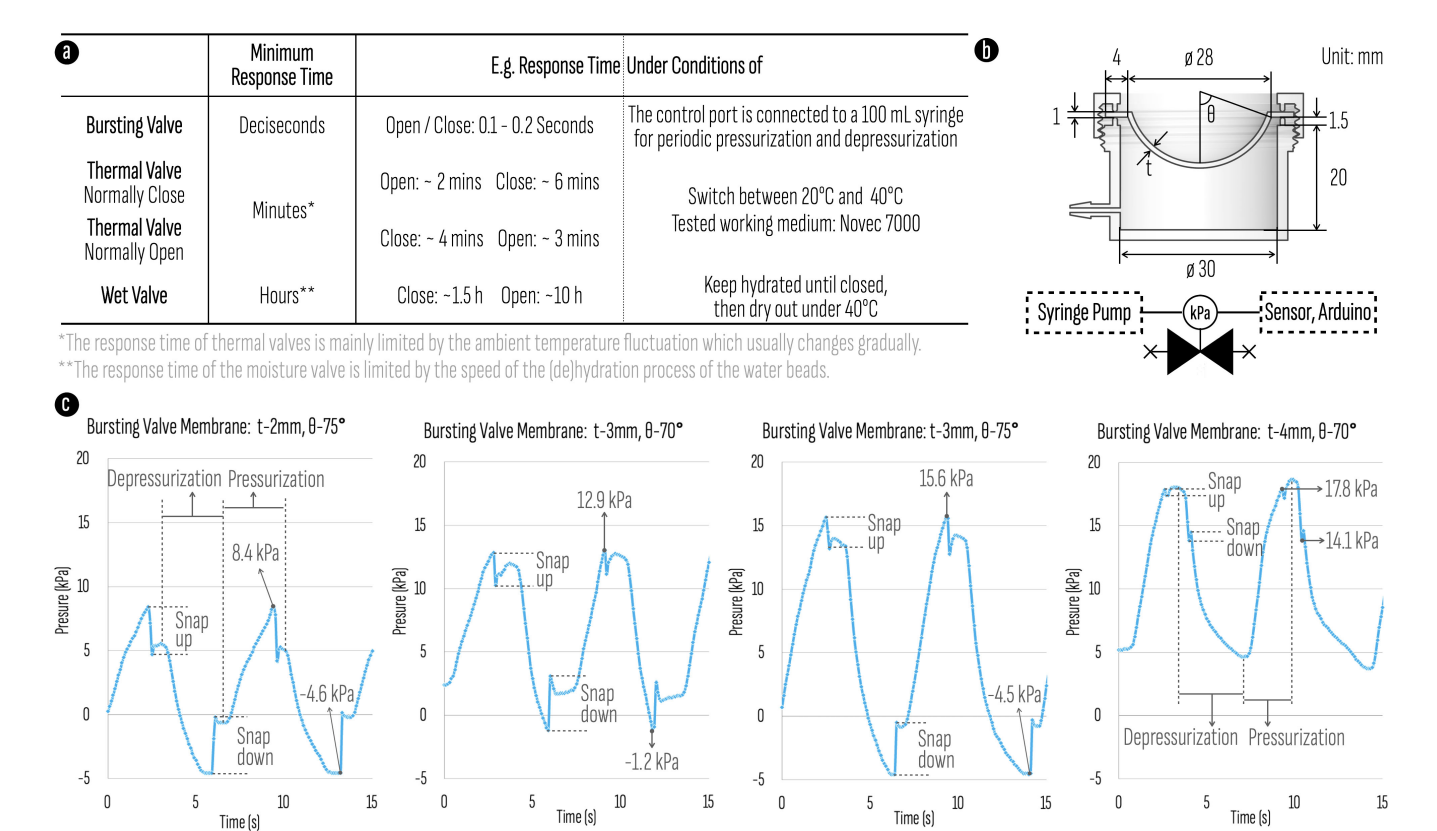


Figure 12: The performance evaluation results of the energy utilization valves. a). Summary table of the results. b). The geometry (top) and the experiment setup (bottom) of the bursting valve. c). The test results of bursting valves with different bistable membranes. The abrupt variations in air pressure during pressurization/depressurization are attributed to the bistable membrane's rapid snap up/down movement.

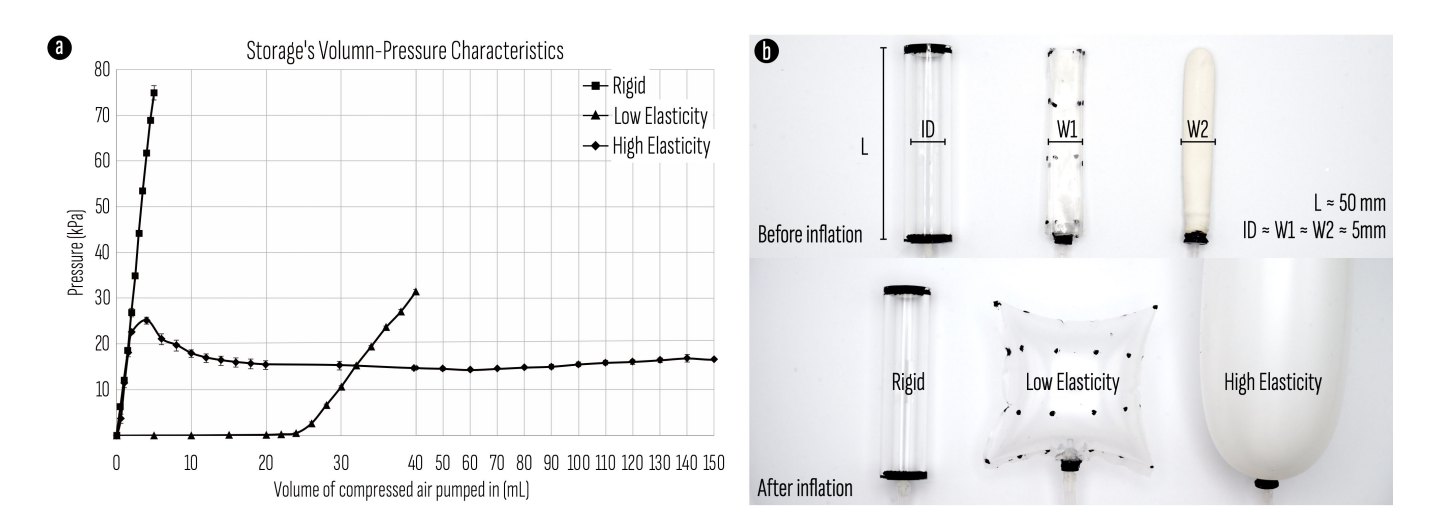


Figure 13: a). The relation of "volume of compressed air pumped in" and pressure of the sample rigid, low elastic, and highly elastic storage. b). The dimension of the tested samples, and the comparison of them before and after being inflated.

3.2.4 Performance Evaluation and Comparison of Valves. The response time of the valves was primarily evaluated and the minimum response time magnitude and example response time under specific conditions are summarized in Figure 12.a.

The bursting valve is capable of reacting within decise conds once the air pressure threshold is reached due to the bistable membrane. While there are many factors that can influence the threshold pressure [33, 68, 77], we primarily adjust the *membrane thickness t* and *central angle* θ to achieve differential thresholds (Figure 12.b). The threshold pressure and response curves are depicted in Figure 12.c. The rapid and distinct transitions in air pressure observed during both pressurization and depressurization processes are attributed to the swift snap up and snap down movements of the bistable membrane. These movements dictate the response speed of the bursting valve.

Although the NC thermal valve uses a t=2 mm, $\theta=75^{\circ}$ C bistable membrane, it doesn't rely on the abrupt bistable phenomenon to operate. As to the NO thermal valve and moisture valve, they both feature a thin non-bistable membrane. Although the thermal valve responded within minutes and the moisture valve took hours to

respond under our test conditions, their response times in real-world applications will depend on ambient conditions, such as the speed of temperature fluctuations for thermal valves and moisture fluctuations for moisture valves. Also, the threshold temperature of the thermal valve is mainly decided by the LBL types.

3.3 Storages for Energy Accumulation

Storage units made of different materials will exhibit different volume and pressure characteristics. The testing results of a rigid acrylic cylinder storage (ID 10 mm, L 50 mm), a square low elasticity thermal plastic storage (50 mm x 50 mm, 10 mm x 50 mm after folding), and a rectangular high elasticity rubber storage (10 mm x 50 mm) are plotted in Fig. 13.a. It is evident that the rigid storage is suitable for use cases where rapidly building up pressure is a priority, but only a limited volume of compressed air can be efficiently accumulated. On the other hand, highly elastic storage is ideal for applications requiring a high volume of compressed air, but its pressure builds up slowly. A low elastic storage is a more balanced choice for both metrics.

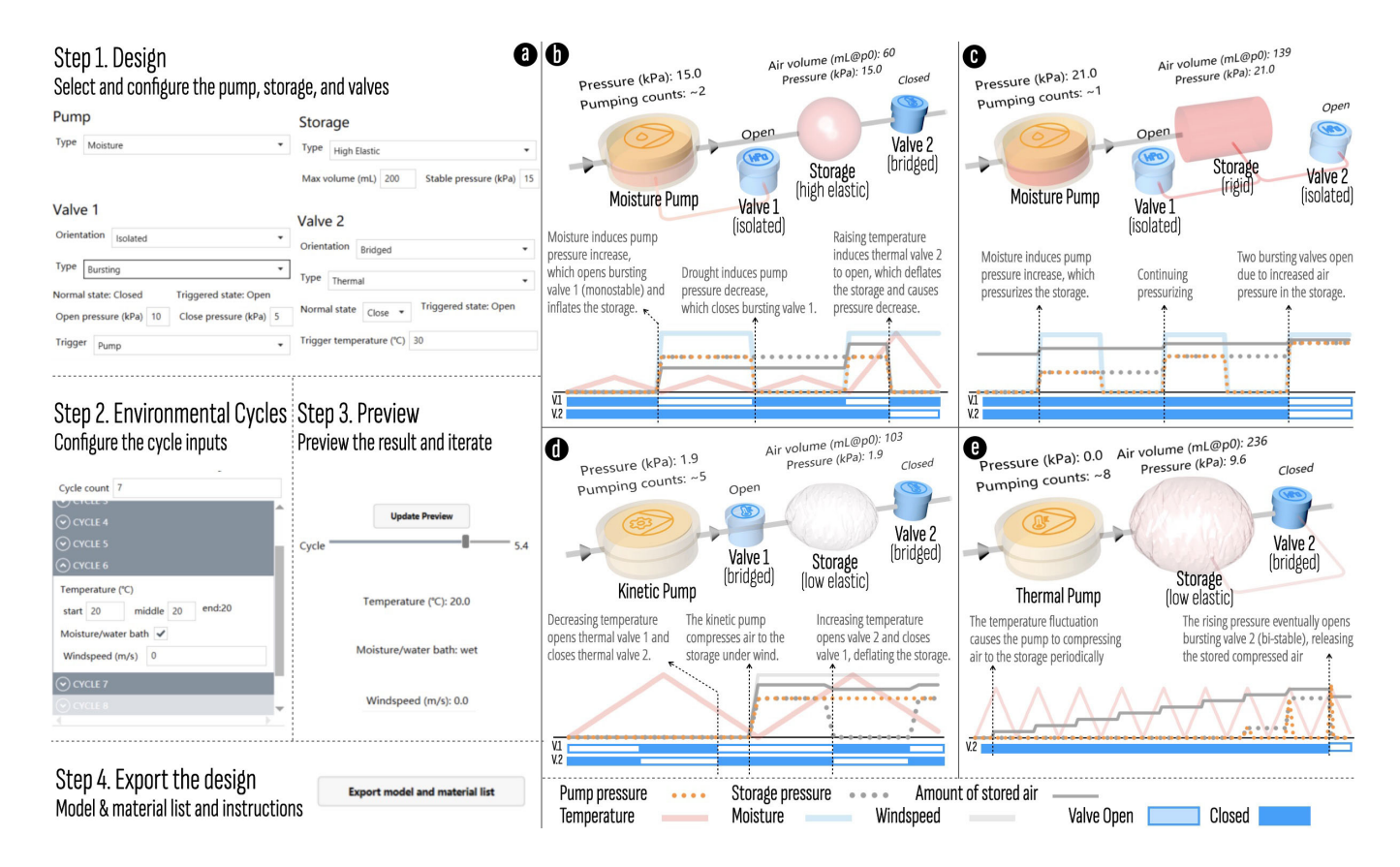


Figure 14: Design tool interface. a). The GUI that allows users to input design configurations. b). Visualization and simulation based on the design configuration selected in (a). c-e). Other visualization examples based on alternative design configurations. For all previews shown in (b-e), the volume changing of the components is visualized by three-dimensional models; the internal pressure changes of the pump and storage are demonstrated through the varying transparency of the red fill; the open or closed state of the valves is signaled by their transition between translucent and solid appearances. In (b-e), we also provide the corresponding diagrams at the bottom to visualize input stimuli and data output along the temporal dimension.

4 DESIGN TOOL

We developed a design tool to guide users through the design and fabrication process of Sustainflatable system. The design tool enables the users to explore different configurations and structures of the system with a simple GUI. It also provides a preview of the system's working procedure reacting to the environment changes, which will helps users better understand and iterate the function of the designed system. Lastly, the tool can export corresponding model and material list to facilitate prototyping of the system. We developed the design tool on Rhino 7 Grasshopper platform. We introduced the user workflow and implementation in the following sections.

4.1 User workflow

The overall user workflow of the design tool are introduced in the following four steps.

4.1.1 Step 1. Design a Sustainflatable system. First, the user designs a Sustainflatable system by configuring a few pneumatic components based on a template. In this version, we pre-defined a template with four elements connected in series: a pump, valve1, storage, and valve2, which covers most of the system design we have explored and also maintains a relatively simple structure (Fig. 14.b-e). For each component, users can configure basic type and most of the related functional parameters (Fig. 14.a). Specifically for the valve, we provides two orientations (Bridged and isolated orientations in Fig. 14.b) to extend the design space of the system structure. The user can get a real-time structure diagram in three-dimensional preview window in the design tool.

4.1.2 Step 2. Configure the environmental cycle inputs. Next, the user configures the environmental condition with a series of cycles. Here, a cycle refers to a shortest period of environmental change that may lead to a periodic working processes of the system, which contains a round-change of temperature and a constant moisture and wind condition. (For example, a day with a lower temperature at early morning and midnight, a higher temperature at noon, and a relative constant rain and wind condition may constitute a cycle.) Users can carefully design the condition of each cycle in the design tool (Fig. 14.a).

4.1.3 Step 3. Generate preview results. Then, the user hits the 'Update Preview' button, slides the timeline to watch the preview of the system's working procedure corresponding to the cycles of the environmental conditions from step 2. The design tool provides previews of a few status parameters, e.g., the pressure and the pumping volume of the pump, the pressure and the air amount of the storage, and the states of the valves. The changing process of the parameters, as well as and their logical correlation with the environmental conditions, preview the primary functionality of the system design (Fig. 14.b-e), which are expected to provide an intuitive understanding for the users before their actual application. Users can go back to step 2 to iterate the system design if the previewed function is not satisfying.

4.1.4 Step 4. Export the components list. Upon completing the design of the Sustainflatable system, the user can click on the "Export model and material list" button. Subsequently, the design tool will

provide relevant instruction manual detailing the material lists, fabrication methods and assembly process of the utilized components. These instructions can also be found in the supplementary materials provided.

4.2 Implementation

The implementation of the computational model for the design tool follows the main workflow in Fig. 15a. Here, we first interpreted the inputs of environment cycles from the users into a group of environmental factor functions $\{e_i(t)\}$, which describes the changing process of the environment factors in the algorithm, including temperature T(t), moisture mo(t), and wind speed $v_{\mathrm{wind}}(t)$ in this version. Next, based on our analytical pump models, we transformed the above $\{e_i(t)\}$ into a unified actuated pressure function $p_a(t)$, served as a pneumatic pressure input applied on the pump in the system by the environment factors. Then, we solved a group of system status parameters $\{s_i(t_n)\}$ as the output preview results at time t_n , which describe the status of each component in the system with a few variables defined in Fig. 15.b. This procedure works on an iterative algorithm to simulate the pneumatic quasi-static process of the gas, which solves each $\{s_i(t_n)\}$ based on previous system status parameters $\{s_i(t_{n-1})\}$, current environmental factors $e_i(t)$, and current actuated pressure $p_a(t_n)$. We detailed the above workflow in the following three parts:

4.2.1 Analytical models for the pump, storage, and valve. We used analytical models to quantify the relationship of critical physical parameters for each type of components, embedding the models in the algorithm as computational models for the system.

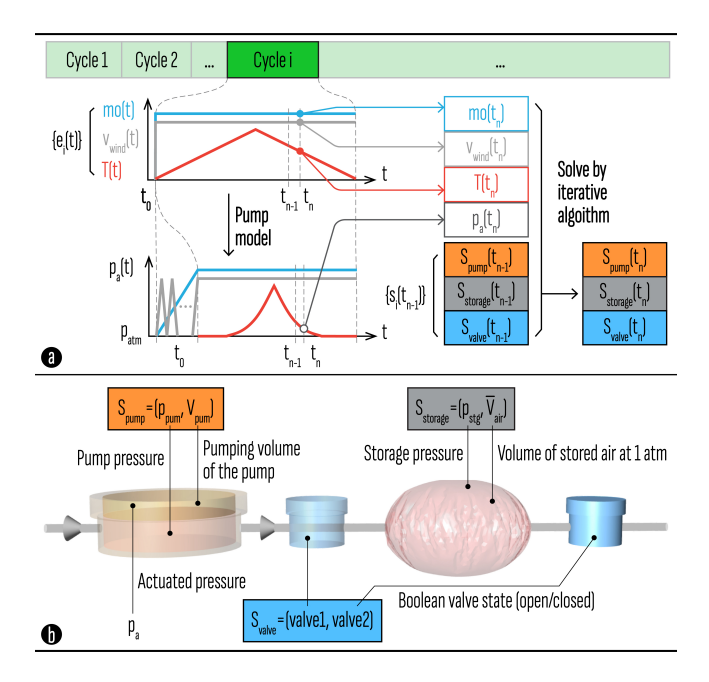


Figure 15: Design tool implementation. a). The main workflow of the computational model of the design tool. b). Definition of the system status parameters used in the computational model.

Table 1: Empirical parameters in the design tool

	Value	Reference
p_{LBL}^*	Formula	techanical data sheet of LBL (e.g. Novec 7000)
p_{moi}^*	128.3 kPa	measurement in Fig. 7.b plus $p_{\rm atm}$ (101.3kPa)
$\lambda_{ ext{win}}^*$	7.7×10^{-2}	linear regression ($r^2 = 0.95$) according to Fig 7.e
$U^*_{ m pum}$	56.5 mL	pump mechanical design
$V_{ m pum}^*$	22/29/20 mL	measurement in Fig. 7.b
$V_{ m stg}^*$	Customized	storage design or measurements
k^* (rigid)	0.58	linear regression ($r^2 = 0.998$) according to Fig. 13.a
k^* (low elastic)	0.52	linear regression ($r^2 = 0.999$) according to Fig. 13.a
$P_{ m els}^*$	167.3 kPa	estimation according to Fig. 13.a plus $p_{\rm atm}$

The pump model is used to solve the actuated pressure p_a of each type of the pump according to the corresponding environmental factor. Given by Equ. 1-3, p_a for thermal pump is assumed to be the saturated vapor pressure $p_{\rm LBL}^*(T)$ of the LBL under temperature T when larger than $p_{\rm atm}$, for moisture pump, is assumed to be the maximal pressure $p_{\rm moi}^*$ of the water beads applied to the pump, and for kinetic pump, to be $p_{\rm atm}$ plus an additional pressure, which is proportional to the square of the wind speed $v_{\rm wind}$ according to Bernoulli's law with an empirical coefficient $\lambda_{\rm win}^*$. In our pneumatic system, p_a serves as either the pressure input applied to the pumps by the environment, or the upper limit of the pressure the pump is able to build in the system, which can be estimated by the maximum pressure measured in section 3.1.4 for the pump.

$$p_a = \max\{p_{\text{atm}}, p_{\text{LBL}}^*(T)\}$$
 (Thermal) (1)

$$p_a = p_{\text{moi}}^*$$
 (Moisture) (2)

$$p_a = p_{\text{atm}} + \lambda_{\text{win}}^* v_{\text{wind}}^2$$
 (Kinetic) (3)

The pump model is also used to solve the status parameters for the pump, given p_a above. Here to simplify the model, we ignored the temperature fluctuation inside the pump. When $p_a > p_{\rm atm}$, the pump is pressurized and tends to maintain a maximal inner pressure $p_{\rm pum}$ under a few physical constraints given by Equ. 4-5, where $U_{\rm pum}^*$ denotes the inherent volume of the pump, $C_{\rm pum}$ is the isothermal product of air pressure and volume depending on the amount of the air inside the pump, and $V_{\rm pum}^*$ denotes the maximal pumping volume. When $p_a \leq p_{\rm atm}$, we assumed that the pump immediately breath in air from outside and return to initial state $(p_{\rm pum} = p_{\rm atm}, V_{\rm pum} = 0)$.

$$\max_{V_{\mathrm{pum}}} p_{\mathrm{pum}} \tag{4}$$

$$s.t. \begin{cases} p_{\text{pum}} \times (U_{\text{pum}}^* - V_{\text{pum}}) = C_{\text{pum}} \\ 0 \le V_{\text{pum}} \le V_{\text{pum}}^* \\ p_{\text{atm}} < p_{\text{pum}} \le p_a \end{cases}$$
 (5)

The storage model is used to solve the status parameters for three kinds of storage. The rigid storage is assumed to follow an isochoric process when working. Based on the Ideal Gas Law, we used Equ. 6 to solve the storage pressure $p_{\rm stg}$ given the volume of inside air at standard atmospheric pressure $\bar{V}_{\rm air}$, where $V_{\rm stg}^*$ denotes the inherent volume of the storage and k^* is a correction factor to compensate for the measurement error and slightly elastic expansion of $V_{\rm stg}^*$.

Algorithm 1 Pneumatic quasi-static process simulation

Input: $\{s_i(t_{n-1})\}, \{e_i(t_n)\}, p_a|_{\{e_i(t_n)\}}$ Output: $\{s_i(t_n)\}$

1: **if** $p_a > p_{\text{stg}} \land \text{ valve1}$ is used and open **then**

2:
$$V_{\text{new}} \leftarrow \bar{V}_{\text{air}}$$
 \Rightarrow Storage inflates

3: repeat

4:
$$V_{\text{new}} \leftarrow V_{\text{new}} + \Delta V_{\text{new}}$$

5: Solve
$$p_{\text{stg}}$$
 by Storage Model Equ.6-8 $|_{\bar{V}_{\text{air}} \leftarrow V_{\text{new}}}$

6:
$$p_{\text{pum}} \leftarrow p_{\text{stg}}, C_{\text{pum}} \leftarrow C_{\text{pum}} - p_{\text{atm}} \Delta V_{\text{new}}$$

7: Try to solve
$$V_{\text{pum}}$$
 by $Pump Model Equ. 4-5 |_{p_a,p_{\text{pum}},C_{\text{pum}}}$

8: **until**
$$\nexists (p_{\text{pum}}, V_{\text{pum}})$$
 s.t. Pump Model Equ.4-5

9: **else if**
$$p_a \le p_{\text{atm}}$$
 then \triangleright Pump breathes in air

10:
$$(p_{\text{pum}}, V_{\text{pum}}) \leftarrow (p_{\text{atm}}, 0)$$

Solve
$$(p_{pum}, V_{pum})$$
 by $Pump Model Equ. 4-5 | p_a$

13: end if

if Valve2 is a bursting valve then

16: Solve
$$\bar{V}_{air}$$
 by Storage Model Equ.6-8| $p_{stg} \leftarrow p_{valve off}$

17: else

18: Solve
$$\bar{V}_{air}$$
 by Storage Model Equ.6-8| $p_{stg} \leftarrow p_{atm}$

19: end if

20: end if

21:
$$s_{\text{pump}}(t_n) \leftarrow (p_{\text{pum}}, V_{\text{pum}})$$

22:
$$s_{\text{storage}}(t_n) \leftarrow (p_{\text{stg}}, \bar{V}_{\text{air}})$$

23:
$$s_{\text{valve}}(t_n) \leftarrow Valve\ Model|_{\{e_i(t_n)\},s_{\text{pump}}(t_n),s_{\text{storage}}(t_n)}$$

The soft storage is assumed to follow an isobaric process before reaching $V_{\rm stg}^*$, and follow an isochoric process as the rigid storage after, given by Equ. 7. The elastic storage performs a more complex expansion process in the experiments according to Fig. 13.c, which is simplified as an isobaric process holding an empirical stable pressure $p_{\rm els}^*$, only when p_a is larger than $p_{\rm els}^*$, given by Equ. 8.

$$p_{\rm stg} = \frac{RT}{V_{\rm stg}} n_{\rm stg} = k^* \frac{p_{\rm atm}}{V_{\rm stg}^*} \bar{V}_{\rm air} \tag{Rigid}$$

$$p_{\rm stg} = \begin{cases} p_{\rm atm}, & (\bar{V}_{\rm air} < V_{\rm stg}^*) \\ k^* \frac{p_{\rm atm}}{V_{\rm stg}^*} \bar{V}_{\rm air}, & (\bar{V}_{\rm air} \ge V_{\rm stg}^*) \end{cases}$$
 (Low Elastic) (7)

$$p_{\text{stg}} = \begin{cases} p_{\text{atm}}, & (p_a < p_{\text{els}}^* \lor \bar{V}_{\text{air}} = 0) \\ p_{\text{els}}^*, & (p_a \ge p_{\text{els}}^* \lor \bar{V}_{\text{air}} > 0) \end{cases}$$
(Highly Elastic) (8)

The operational states of the thermal and moisture valves are determined according to the simple binary environmental condition. The bursting valve is assumed to follows the hysteretic characteristic[68], which uses two critical pressure thresholds at open and closed states respectively.

All variables marked with an asterisk (*) may vary empirically depending on the customization of the situation, such as the choice of materials, mechanical design, and so forth. The values of these variables as implemented in our design tool are provided in Table 1. These values can also be modified directly within the program. For clarity, we would like to note that all pressure-related variables in our implementation use absolute pressure for computation.

4.2.2 Interpretation of environment cycles. The design tool interprets the environment cycles input from the users to a group of environmental factor functions $\{e_i(t)\}$ for further actuated pressure function $p_a(t)$ computation. As shown in Fig. 15a, the temperature in one cycle is assumed to change linearly and then produces a continuous pressure changes of p_a according to Equ. 1 The moisture and the wind speed are assumed to keep constant in one cycle, producing a constant p_a according to Equ. 2-3. While, between two cycles, the moisture change is interpreted as a linear changing

process of p_a , and the wind speed change is interpreted as an oscillating process of p_a until the inside pressure reaches a stable value, which imitates the pumping process actuated by the rotation of the windwheel.

4.2.3 Iterative algorithm of pneumatic quasi-static process simulation. We used an iterative Algorithm 1 to solve the system status $\{s_i(t_n)\}$ given every environmental factors $\{e_i(t_n)\}$ and actuated pressures $p_a(t_n)$. At each time step t_n , the program repeatedly runs algorithm until the system status remains stable based on the quasi-static process assumption.

5 APPLICATION EXAMPLES

The Sustainflatable system is designed to be versatile and adaptable, making it suitable for deployment in various settings, whether indoors or outdoors. It is also autonomous, meaning that it does not require constant human intervention or monitoring. In this section, we present several examples of how the system can be used in a backyard garden context (Fig. 16). These concepts serve to illustrate the potential of our technique and inspire HCI researchers and designers to develop even more innovative and sophisticated applications in a wide range of scenarios.

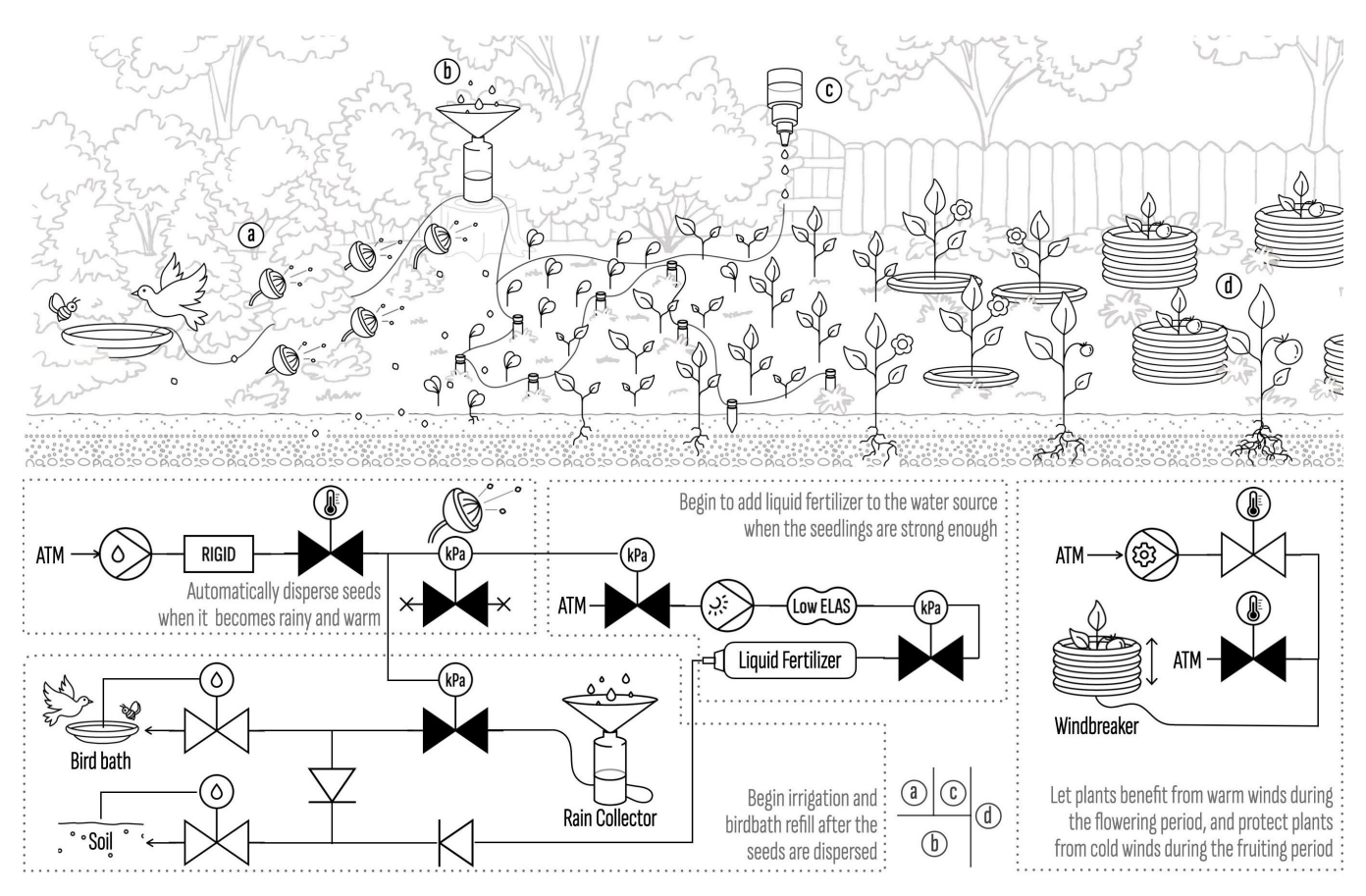


Figure 16: Overview of application examples. a). Automatic seeds ejection under the right time and conditions. b). Subsequent self-feedback irrigation and bird baths fill. c). Appropriately timed fertilization when the seedlings are strong enough. d). Self-regulating plant insulation for flowering and fruiting period.

5.1 Automatic Seeds Ejection under Suitable Conditions

Some plants have evolved unique and effective seed dispersal mechanisms. For example, when squirting cucumber's fruit is ripe, any slight touch or disturbance can cause it to burst open, ejecting the seeds inside with a forceful squirt This mechanism is an adaptation that allows the plant to disperse its seeds over a wider area, increasing the likelihood of successful germination and growth.

Inspired by natural phenomena, we have developed an automatic seed dispersal system, illustrated in Fig. 17.a and 14.b. Compared to the design shown in Figure 14.b, the current design has omitted valve 1, which was used to limit the maximum air pressure and prevent damage to the water beads. Additionally, a rigid storage has been adopted in this demonstration to allow for faster pressure accumulation.

Imagine a garden in a temperate continental climate zone, where winters are cold and dry but springs are characterized by frequent rain. In the system, a moisture pump will compress air towards the storage unit when spring starts, accumulating pressure (Fig. 17.b1). The successive thermal valve ensures that compressed air is only released to the bursting valve when it is warm enough (Fig. 17.b2). Once the necessary pressure has been accumulated and the temperature is favorable, the bursting valve ejects the seeds with an initial velocity of approximately $\sim 4 \text{m/s}$ (Fig. 17.c). The bursting valve features a customized body and a customized membrane [33] that enables faster snap-through speed. Additionally, a small shelter

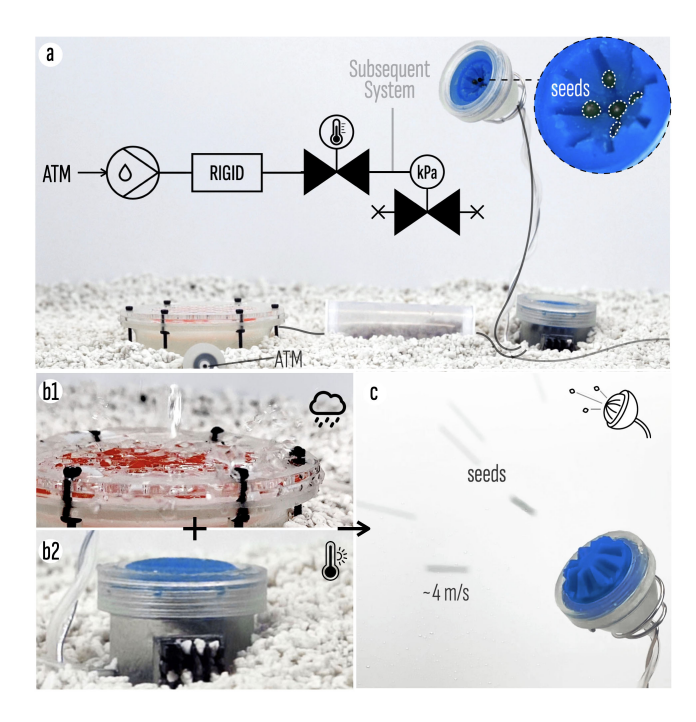


Figure 17: Automatic Seeds Ejection Under Suitable Conditions. a). The system overview. b1) The moisture pumps begin to operate when it becomes rainy. b2) The thermal pump gradually opens when the weather is warm. c) Seeds are dispersed when both conditions are met.

structure may be added to the bursting valve to make it rainproof. Multiple bursting valves can be connected in parallel to disperse more seeds.

5.2 Self-feedback Irrigation and Bird Baths Fill

Timely irrigation plays a crucial role in successful seed germination. By watering the soil at the right time, we can provide sufficient moisture for the seeds to absorb and start growing. Moreover, placing bird nests, bee houses, and bird baths in the garden can attract pollinators and predators of pests [60][54]. By creating a welcoming environment for these beneficial creatures, we are promoting a healthy and sustainable ecosystem in the garden.

As shown in Fig. 18, the rainwater collector is controlled by a bursting valve which will open simultaneously with the seeding dispersal (Fig. 18.b1 to b2). This will enable rainwater to flow into the irrigation and birdbath fill system (Fig. 18.d1, c1). Successive moisture valves will halt the irrigation and refill processes once the soil is sufficiently moist and the birdbath is full (Fig. 18.d2, c2), and

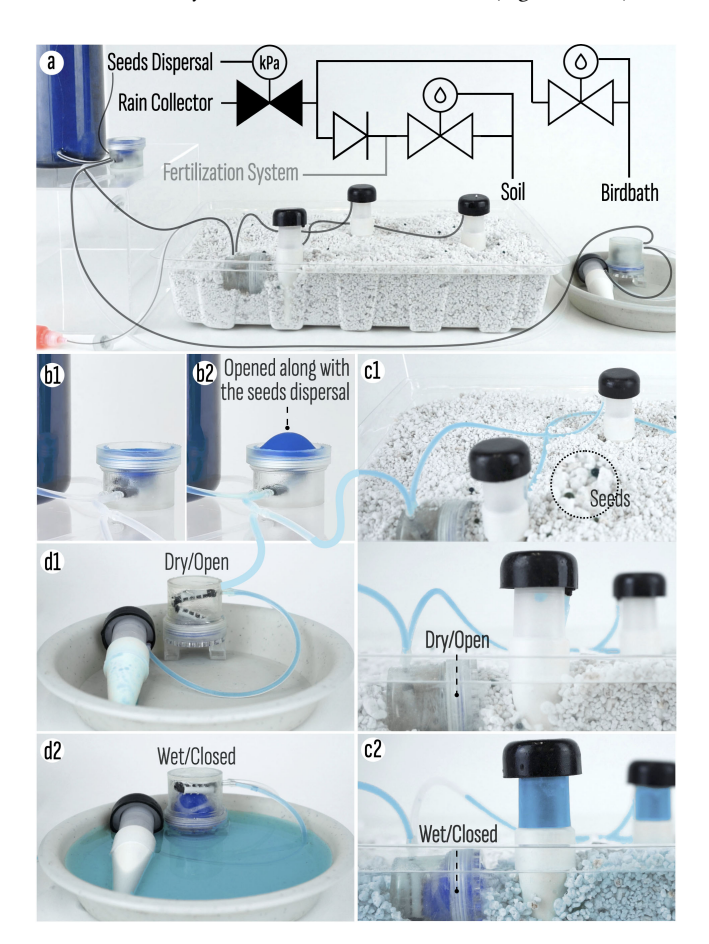


Figure 18: Self-feedback irrigation and bird baths refill. a). The system overview. b) The bursting valve opens simultaneously with the seeding dispersal and releases the stored rain water. c1) The irrigation begins. c2) The irrigation stops when the soil is sufficiently moist. d1) The bird bath fill begins. d2). The fill stops when the bird bath is full.

will resume the processes when the soil dries out and the water level in the birdbath drops. Due to the relatively slow response time of the moisture valves, we have incorporated ceramic porous rods to prevent over-irrigation and over-refilling by allowing water to seep out gradually. In addition, to prevent contamination of the birdbath refill system by the fertilizer which will be added later, a check valve is installed in front of the mixing point.

5.3 Appropriately Timed Fertilization

Fertilizers can promote plant growth and ensure optimal yields. However, the timing of fertilizer application is crucial, and applying fertilizer at the wrong time can have negative consequences. For instance, applying fertilizer to a newly germinated seedling can lead to fertilizer burn, a condition where the fertilizer salts build up around the delicate root system of the young plant, causing damage or even death [63].

The appropriately timed liquid fertilizer distribution system we developed is depicted in Fig. 19 and Fig. 14.e. At the same time as the seeding dispersal, the bursting valve opens, unblocking the inlet of the thermal pump and allowing it to generate compressed air based on daily temperature fluctuations (Fig. 19.b1, b2). After a specified number of days, when the seedlings are strong enough, the second bursting valve bursts, allowing the compressed air to squeeze the liquid fertilizer out and mix it with rainwater before being applied to the plants via the irrigation system (Fig. 19.b3).

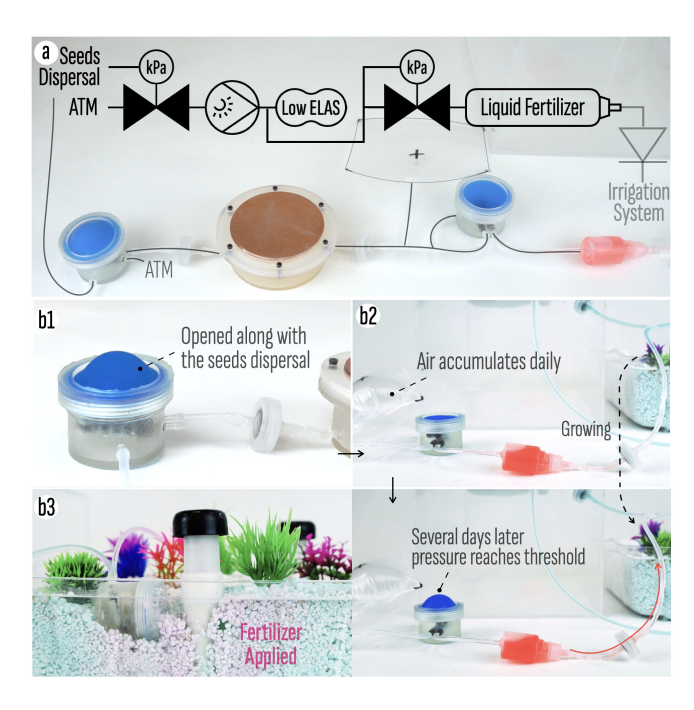


Figure 19: Appropriately Timed Fertilization. a). The system overview. b1). The bursting valve opens along with the seeding dispersal, allowing the subsequent thermal to begin operating. b2). Air accumulates daily as temperature fluctuates and the seedlings are growing. b3). The fertilizer is squeezed out and added to the irrigation system when the seedlings are strong enough.

To prevent the backflow of the irrigation rainwater, a check valve is installed in front of the mixing point. The waiting time before distributing the fertilizer can be estimated and optimized using our design tool ahead.

5.4 Self-regulating Plant Insulation

Wind is an important factor in the growth and survival of plants, providing several benefits such as promoting pollination [12], improving transpiration [27], and pest control [59]. However, a cold,

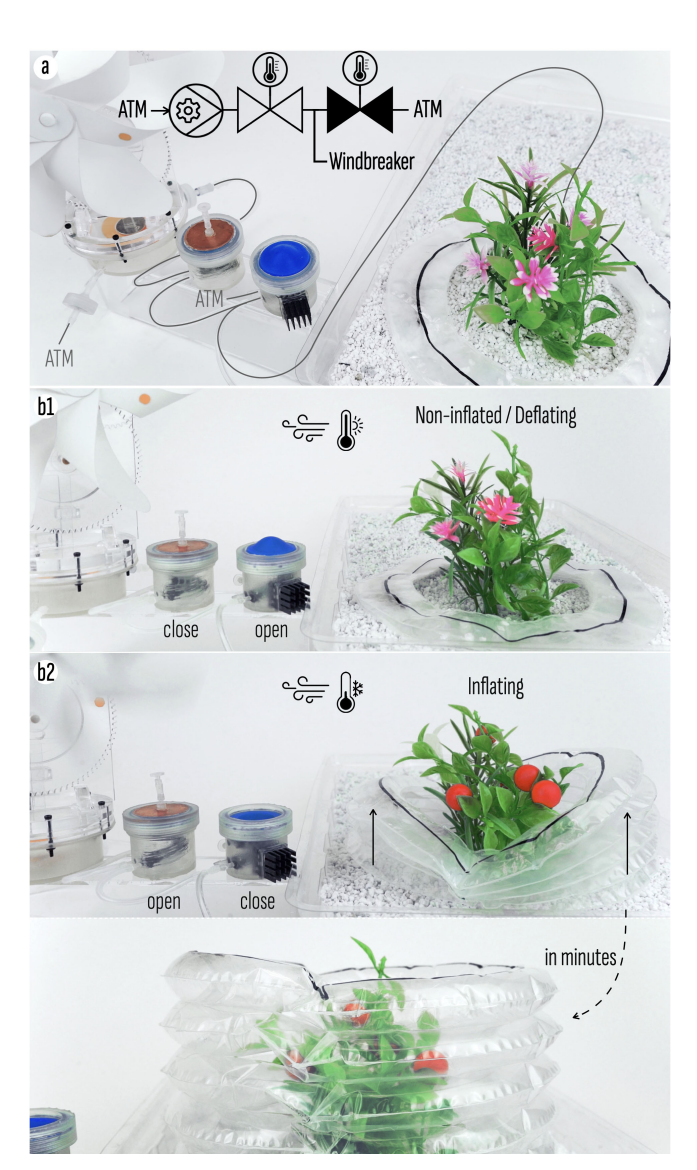


Figure 20: Self-regulating plant insulation. a). The system overview. b1). The windbreaker will not inflate during warm weather. The high air pressure accumulated inside the pump restricts the movement of its thin membrane, which prevents the windmill from turning with the wind. b2). The windbreaker will inflate and protect the plant during cold windy days.

strong wind in the late fall can have negative effects on plants. The low temperatures and high wind speeds can cause excessive water loss through transpiration, leading to dehydration and wilting. Additionally, the harsh winds can cause delayed ripening or even chilling injury to the fruits [45].

To harness the advantages of wind while mitigating potential hazards, we have implemented a self-regulating insulation system, as demonstrated in Fig. 20 and Fig. 14.d. The wind pump can be positioned to face the prevailing wind direction during autumn. During warm weather before the fall, the NO thermal valve closes while the NC thermal valve opens. This prevents air from being pumped into the inflatable windbreaker, enabling the plants to benefit from the wind (Fig. 20.b1). When there is cold wind, the NO thermal valve opens while the NC thermal valve closes and the wind pump will operate, gradually inflating the windbreaker and shielding the plants from the wind (Fig. 20.b2). If the temperature fluctuates and rises above the threshold, the windbreaker can slowly deflate. This automated process ensures that the windbreaker provides the necessary protection to the plants during inclement weather without many human interventions.

6 DISCUSSION, LIMITATION AND FUTURE WORK

6.1 Beyond Energy Sustainability

The Sustainflatable system is good at harnessing renewable energy. Here, we would like to discuss further regarding the material sustainability of it form these three aspects:

Reusing and Recycling materials can reduce waste and decrease the need for virgin materials. Our pumps and valves are designed with a consistent design language. As a result, they share many interchangeable parts that can be reused in reconfigurations, contributing to a more sustainable approach. Additionally, the Sustainflatable components have only a few material compositions, making it much simpler to disassemble and recycle compared to an electronic energy utilization system.

Biodegradability. Although not all of the materials used in the prototypes of our system are biodegradable – mainly due to the need of rapid iteration – our system can potentially be fabricated with biodegradable materials. The rigid components may be 3D-printed with biodegradable polymers, such as polyvinyl alcohol (PVA) that can be easily dissolved [3], or polylactic acid (PLA) that is also biodegradable [5]. The silicone membranes may be replaced by bio-based synthetic elastomers for various shore hardness [78]. We envision our system can be produced with biodegradable components to further contribute to a sustainable future.

Material Safety. Our Sustainflatable components primarily consist of commonly used polymers, elastomers, hydrogels, and wood, which are considered non-toxic or have limited toxicity compared to substances like heavy metals in electronic devices or even many common household chemicals. The only relatively unique material is the LBL inside the thermal pump and valve, among which the Novec LBLs are generally considered to have low toxicity and has been adopted in designing thermal-pneumatic actuators and interfaces by many researchers [22, 39, 50, 52, 53, 69]. To achieve functional thermal pump and valve at a lower threshold, we also

proposed using other LBLs like acetaldehyde ³ and 1,2-Butadiene ^{4 5}, which have no known critical hazards at low amounts when handled properly according to the SDS. Acetaldehyde is a natural substance found in many foods, such as coffee, bread, and ripe fruit, and is produced by plants [83]. Furthermore, the amount of LBL required for the pump and valve is minimal, and it is confined within the pump or valve. Nevertheless, we are looking forward to the development of new LBL or low temperature-responsive materials to further extend the working temperature range while maintaining even higher standard material safety.

6.2 Long-Term Operating Performance

Pressure Maintenance. For application scenarios spanning extensive time frames, maintaining the airtightness of the system is crucial for efficient energy collection and accumulation. In general, pumps, valves, and rigid storage units can provide satisfactory airtightness when properly assembled, with a typical air pressure loss of ~ 0.3 kPa per day. However, storage units with low elasticity may experience a higher pressure loss over time. As an example, we studied a 50 mm x 50 mm square airbag crafted from 1 mm thick TPU film. The pressure drop over 24 hours fluctuated between 0-0.8 kPa as the internal pressure escalated from 0-20 kPa (in 5 kPa increments). This variability could clarify why the 24-hour cycle thermal pump experiment took longer to build pressure compared to the 180 s cycle experiment. Regarding highly elastic storage, the pressure remains relatively stable during the plateau period as shown in Fig. 13.a. However, air loss can still occur due to the permeable nature of rubber. Based on our tests, an inflated 100 mL rubber latex balloon may lose ~ 15 mL of air per day. This air loss can be significantly reduced to 2-5 mL per day when manually coated with HiFloat⁶, depending on the quality of the coating. In conclusion, when selecting low or high elastic storage materials, those with lower permeability coefficients are preferred. If such materials are not available, post-processing methods may be employed to reduce the permeability.

Pump durability. As the components that cycle most frequently, all the pumps generally display robust iterative performance. Kinetic Pump: We conducted a test in which the piston cycled up and down ~ 15 times per minute. After 12 hours, encompassing over 10,000 cycles, the pump remained functional. Moisture Pump: The water beads employed in the moisture pump can be used repeatedly; we've successfully utilized some for more than 50 cycles. However, these beads soften and may crush under high air pressure when swelled, which defines the moisture pump's maximum pressure. For optimal pump performance, crushed beads should be replaced. In many scenarios, such as when connected to a bursting valve, the moisture pump doesn't reach its maximum pressure, thus preventing bead crushing. Thermal Pump: We have observed that the LBL bladder might not be able to fully reversible even at low temperatures after long-term use (~ 4 weeks or more), which can diminish the thermal pump's performance. While this situation may not occur frequently, if the performance is significantly impaired, the LBL bladder can be drained and refilled.

³Acetaldehyde safety data sheet

⁴1,2-Butadiene safety data sheet 1

⁵1,2-Butadiene safety data sheet 2

⁶HiFloat Coating

6.3 Design Tool Optimization

The current design tool provides users with the ability to explore different system designs and understand system functions through a preliminary simulation and preview. However, there is room for improvement.

Since some of the analytical models in the design tool integrate coefficients and other constants derived from our empirical experimental data, the comprehensiveness and accuracy of the physical experiments can affect the accuracy of the preview. To increase the accuracy of the preview function, we suggest two improvements for future study. Firstly, more experimental data can be collected under different controlled conditions, such as varying temperature, moisture, and wind conditions, as well as long-term natural environmental conditions. This will allow us to further improve the performance of the analytical models. Secondly, variations in size, mechanical design, and choices of environmentally responsive materials can be considered, experimented with, and embedded in the computational models in the design tool. Lastly, we can include the waterfall kinetic pump in the design tool to provide users with more options for their designs.

Additionally, to make the tool more applicable to various scenarios, we can consider extending the algorithmic functionality. Currently, the tool implements the most representative templates of the Sustainflatable system structure. In the future, more combinatorial configurations of the components could be included, such as connecting more components in series or parallel. These additions would expand the design possibilities, provide previews of functions with more complicated logic, and allow a better understanding of more complex system design. Moreover, modeling the system to elucidate the underlying physics can also further increase accuracy and universality, and enable optimization to maximize energy-harnessing performance [74].

6.4 Broader Adaptability, Broader Impact

To push the Sustainflatable system even more versatile, we can explore more mechanisms to harness other forms of renewable energy. For instance, the kinetic pump can be modified with a lever structure to collect tidal and wave energy [11, 17], and a small compost pile can be integrated to the thermal pump to harvest energy from microbial decomposition [8, 30]. Similarly, we can develop new mechanisms to leverage these new energy sources as the environmental stimuli to trigger the valve as well.

Additionally, we can further expand the potential impact of the Sustainflatable system by persistently exploring its applications in both outdoor and indoor environments. The system's electronic-free and waterproof design, coupled with its ability to operate autonomously, make it an ideal solution for various in wild applications. To achieve this, we could work towards a more integrated and compact design while utilizing more aforementioned biodegradable and environment-friendly materials. In the future, we may envision deploying these systems in wild to aid in afforestation, environment monitoring, and wildlife shelter distribution, among other applications.

Furthermore, there are numerous forms of ambient energy related to human activities that we can harness. For instance, we might design a wearable system that harvests wind energy produced during running to power the deformation of pneumatic clothing, thereby aiding in temperature regulation and heat dissipation. Alternatively, we could develop a humidity control system for homes or greenhouses that is powered and controlled by moisture levels. Another possibility is to deploy a temperature regulation system for home kitchens or chemical storage facilities in factories, which is powered and controlled by temperature fluctuations. In summary, the continued development and exploration of renewable energy sources, coupled with innovative indoor and outdoor applications of the Sustainflatable system, can pave the way for new and inventive approaches to implementing sustainable technology.

7 CONCLUSION

In conclusion, the Sustainflatable system offers a sustainable solution to power and control pneumatic interfaces. The system's ability to harvest renewable energy sources, convert the energy into compressed air, and store it for later use in a programmable and intelligent way, make it a cost-effective, energy-efficient and environmentally friendly alternative to traditional electric pumps and valves. The system's electronic-free design, incorporating customized energy harvesting pumps, storage units with variable volume-pressure characteristics, and tailored valves that operate autonomously, demonstrates its ability to significantly improve the sustainability of pneumatic interfaces.

ACKNOWLEDGMENTS

We want to thank Lucas Ding for helping conduct certain experiments. We thank the National Science Foundation Grants (Career IIS-2047912 and CNS-2327014) for supporting this work.

REFERENCES

- [1] Nivedita Arora, Vikram Iyer, Hyunjoo Oh, Gregory D. Abowd, and Josiah D. Hester. 2023. Circularity in Energy Harvesting Computational "Things." In Proceedings of the 20th ACM Conference on Embedded Networked Sensor Systems (SenSys '22). Association for Computing Machinery, New York, NY, USA, 931–933. https://doi.org/10.1145/3560905.3568106
- [2] Akash Badshah, Sidhant Gupta, Gabe Cohn, Nicolas Villar, Steve Hodges, and Shwetak N. Patel. 2011. Interactive generator: a self-powered haptic feedback device. In Proceedings of the SIGCHI Conference on Human Factors in Computing Systems (CHI '11). Association for Computing Machinery, New York, NY, USA, 2051–2054. https://doi.org/10.1145/1978942.1979240
- [3] Bálint Basa, Géza Jakab, Nikolett Kállai-Szabó, Bence Borbás, Viktor Fülöp, Emese Balogh, and István Antal. 2021. Evaluation of Biodegradable PVA-Based 3D Printed Carriers during Dissolution. *Materials* 14, 6 (March 2021), 1350. https://doi.org/10.3390/ma14061350
- [4] Fiona Bell, Latifa Al Naimi, Ella McQuaid, and Mirela Alistar. 2022. Designing with Alganyl. In Sixteenth International Conference on Tangible, Embedded, and Embodied Interaction (TEI '22). Association for Computing Machinery, New York, NY, USA, 1–14. https://doi.org/10.1145/3490149.3501308
- [5] Samarthya Bhagia, Kamlesh Bornani, Ruchi Agrawal, Alok Satlewal, Jaroslav Ďurkovič, Rastislav Lagaňa, Meher Bhagia, Chang Geun Yoo, Xianhui Zhao, Vlastimil Kunc, Yunqiao Pu, Soydan Ozcan, and Arthur J. Ragauskas. 2021. Critical review of FDM 3D printing of PLA biocomposites filled with biomass resources, characterization, biodegradability, upcycling and opportunities for biorefineries. Applied Materials Today 24 (Sept. 2021), 101078. https://doi.org/10.1016/j.apmt. 2021.101078
- [6] G. W. Brodland and H. Cohen. 1987. Deflection and snapping of spherical caps. International Journal of Solids and Structures 23, 10 (Jan. 1987), 1341–1356. https://doi.org/10.1016/0020-7683(87)90001-1
- [7] Christopher Chen, David Howard, Steven L. Zhang, Youngwook Do, Sienna Sun, Tingyu Cheng, Zhong Lin Wang, Gregory D. Abowd, and HyunJoo Oh. 2020. SPIN (Self-powered Paper Interfaces): Bridging Triboelectric Nanogenerator with Folding Paper Creases. In Proceedings of the Fourteenth International Conference on Tangible, Embedded, and Embodied Interaction (TEI '20). Association for Computing Machinery, New York, NY, USA, 431-442. https://doi.org/10.1145/3374920.3374946

- [8] Wen Yi Chia, Kit Wayne Chew, Cheng Foh Le, Su Shiung Lam, Chelsea Siew Chyi Chee, Mae See Luan Ooi, and Pau Loke Show. 2020. Sustainable utilization of biowaste compost for renewable energy and soil amendments. Environmental Pollution 267 (Dec. 2020), 115662. https://doi.org/10.1016/j.envpol.2020.115662
- [9] Kyung Yun Choi and Hiroshi Ishii. 2021. Therms-Up!: DIY Inflatables and Interactive Materials by Upcycling Wasted Thermoplastic Bags. In Proceedings of the Fifteenth International Conference on Tangible, Embedded, and Embodied Interaction (TEI '21). Association for Computing Machinery, New York, NY, USA, 1–8. https://doi.org/10.1145/3430524.3442457
- [10] Young-Man Choi, Moon Gu Lee, and Yongho Jeon. 2017. Wearable Biomechanical Energy Harvesting Technologies. *Energies* 10, 10 (Oct. 2017), 1483. https://doi. org/10.3390/en10101483
- [11] M. S. Chowdhury, Kazi Sajedur Rahman, Vidhya Selvanathan, Narissara Nuthammachot, Montri Suklueng, Ali Mostafaeipour, Asiful Habib, Md. Akhtaruzzaman, Nowshad Amin, and Kuaanan Techato. 2021. Current trends and prospects of tidal energy technology. Environment, Development and Sustainability 23, 6 (June 2021), 8179–8194. https://doi.org/10.1007/s10668-020-01013-4
- [12] Theresa M. Culley, Stephen G. Weller, and Ann K. Sakai. 2002. The evolution of wind pollination in angiosperms. *Trends in Ecology & Evolution* 17, 8 (Aug. 2002), 361–369. https://doi.org/10.1016/S0169-5347(02)02540-5
- [13] Alexandra Delazio, Ken Nakagaki, Roberta L. Klatzky, Scott E. Hudson, Jill Fain Lehman, and Alanson P. Sample. 2018. Force Jacket: Pneumatically-Actuated Jacket for Embodied Haptic Experiences. In Proceedings of the 2018 CHI Conference on Human Factors in Computing Systems (CHI '18). Association for Computing Machinery, New York, NY, USA, 1–12. https://doi.org/10.1145/3173574.3173894
- [14] Jialin Deng, Patrick Olivier, Josh Andres, Kirsten Ellis, Ryan Wee, and Florian Floyd Mueller. 2022. Logic Bonbon: Exploring Food as Computational Artifact. In Proceedings of the 2022 CHI Conference on Human Factors in Computing Systems (CHI '22). Association for Computing Machinery, New York, NY, USA, 1–21. https://doi.org/10.1145/3491102.3501926
- [15] Christine Dierk, Molly Jane Pearce Nicholas, and Eric Paulos. 2018. AlterWear: Battery-Free Wearable Displays for Opportunistic Interactions. In Proceedings of the 2018 CHI Conference on Human Factors in Computing Systems (CHI '18). Association for Computing Machinery, New York, NY, USA, 1-11. https://doi. org/10.1145/3173574.3173794
- [16] Dylan Drotman, Saurabh Jadhav, David Sharp, Christian Chan, and Michael T. Tolley. 2021. Electronics-free pneumatic circuits for controlling soft-legged robots. *Science Robotics* 6, 51 (Feb. 2021), eaay2627. https://doi.org/10.1126/scirobotics. aay2627
- [17] António F. de O. Falcão. 2010. Wave energy utilization: A review of the technologies. Renewable and Sustainable Energy Reviews 14, 3 (April 2010), 899–918. https://doi.org/10.1016/j.rser.2009.11.003
- [18] Yusheng Feng, Sydney Jaeyoung Seo, Aidan J. Kennedy, Erika Alice Miyajima, and Tsuiyee Ng. 2020. Reuse Plastic for 3D Printing.
- [19] Sean Follmer, Daniel Leithinger, Alex Olwal, Nadia Cheng, and Hiroshi Ishii. 2012. Jamming user interfaces: programmable particle stiffness and sensing for malleable and shape-changing devices. In Proceedings of the 25th annual ACM symposium on User interface software and technology (UIST '12). Association for Computing Machinery, New York, NY, USA, 519–528. https://doi.org/10.1145/ 2380116.2380181
- [20] Juri Fujii, Satoshi Nakamaru, and Yasuaki Kakehi. 2021. LayerPump: Rapid Prototyping of Functional 3D Objects with Built-in Electrohydrodynamics Pumps Based on Layered Plates. In Proceedings of the Fifteenth International Conference on Tangible, Embedded, and Embodied Interaction (TEI '21). Association for Computing Machinery, New York, NY, USA, 1–7. https://doi.org/10.1145/3430524.3442453
- [21] Azmat Gani. 2021. Fossil fuel energy and environmental performance in an extended STIRPAT model. *Journal of Cleaner Production* 297 (May 2021), 126526. https://doi.org/10.1016/j.jclepro.2021.126526
- [22] Martin Garrad, Gabor Soter, Andrew T. Conn, Helmut Hauser, and Jonathan Rossiter. 2019. Driving Soft Robots with Low-Boiling Point Fluids. In 2019 2nd IEEE International Conference on Soft Robotics (RoboSoft). IEEE Press, New York, NY, USA, 74–79. https://doi.org/10.1109/ROBOSOFT.2019.8722812
- [23] Teng Han, Fraser Anderson, Pourang Irani, and Tovi Grossman. 2018. HydroRing: Supporting Mixed Reality Haptics Using Liquid Flow. In Proceedings of the 31st Annual ACM Symposium on User Interface Software and Technology (UIST '18). Association for Computing Machinery, New York, NY, USA, 913–925. https://doi.org/10.1145/3242587.3242667
- [24] Liang He, Gierad Laput, Eric Brockmeyer, and Jon E. Froehlich. 2017. Squeeza-Pulse: Adding Interactive Input to Fabricated Objects Using Corrugated Tubes and Air Pulses. In Proceedings of the Eleventh International Conference on Tangible, Embedded, and Embodied Interaction (TEI '17). Association for Computing Machinery, New York, NY, USA, 341–350. https://doi.org/10.1145/3024969.3024976
- [25] Wolfgang Hilber. 2016. Stimulus-active polymer actuators for next-generation microfluidic devices. Applied Physics A 122, 8 (July 2016), 751. https://doi.org/10. 1007/s00339-016-0258-6
- [26] Richard Leslie Hills. 1996. Power from Wind: A History of Windmill Technology. Cambridge University Press, Cambridge, England. Google-Books-ID: FoVk-fkBV1_8C.

- [27] Cheng-Wei Huang, Chia-Ren Chu, Cheng-I Hsieh, Sari Palmroth, and Gabriel G. Katul. 2015. Wind-induced leaf transpiration. Advances in Water Resources 86 (Dec. 2015), 240–255. https://doi.org/10.1016/j.advwatres.2015.10.009
- [28] Environmental and Energy Study Institute. 2020. Fossil Fuels | EESI. https://www.eesi.org/topics/fossil-fuels/description
- [29] Alexandra Ion, Ludwig Wall, Robert Kovacs, and Patrick Baudisch. 2017. Digital Mechanical Metamaterials. In Proceedings of the 2017 CHI Conference on Human Factors in Computing Systems (CHI '17). Association for Computing Machinery, New York, NY, USA, 977–988. https://doi.org/10.1145/3025453.3025624
- [30] G. Irvine, E. R. Lamont, and B. Antizar-Ladislao. 2010. Energy from Waste: Reuse of Compost Heat as a Source of Renewable Energy. *International Journal of Chemical Engineering* 2010 (June 2010), e627930. https://doi.org/10.1155/2010/627930
- [31] Hiroshi Ishii, Dávid Lakatos, Leonardo Bonanni, and Jean-Baptiste Labrune. 2012. Radical Atoms: Beyond Tangible Bits, toward Transformable Materials. Interactions 19, 1 (jan 2012), 38–51. https://doi.org/10.1145/2065327.2065337
- [32] Vikram Iyer, Hans Gaensbauer, Thomas L. Daniel, and Shyamnath Gollakota. 2022. Wind dispersal of battery-free wireless devices. *Nature* 603, 7901 (March 2022), 427–433. https://doi.org/10.1038/s41586-021-04363-9
- [33] Lishuai Jin, Yueying Yang, Bryan O. Torres Maldonado, Sebastian David Lee, Nadia Figueroa, Robert J. Full, and Shu Yang. 2023. Ultrafast, Programmable, and Electronics-Free Soft Robots Enabled by Snapping Metacaps. Advanced Intelligent Systems n/a, n/a (Feb. 2023), 2300039. https://doi.org/10.1002/aisy.202300039
- [34] Marion Koelle, Madalina Nicolae, Aditya Shekhar Nittala, Marc Teyssier, and Jürgen Steimle. 2022. Prototyping Soft Devices with Interactive Bioplastics. In Proceedings of the 35th Annual ACM Symposium on User Interface Software and Technology (UIST '22). Association for Computing Machinery, New York, NY, USA, 1–16. https://doi.org/10.1145/3526113.3545623
- [35] Cindy Kohtala. 2017. Making "Making" Critical: How Sustainability is Constituted in Fab Lab Ideology. The Design Journal 20, 3 (May 2017), 375–394. https://doi.org/10.1080/14606925.2016.1261504
- [36] Yuhu Liu, Satoshi Nishikawa, Young ah Seong, Ryuma Niiyama, and Yasuo Kuniyoshi. 2021. ThermoCaress: A Wearable Haptic Device with Illusory Moving Thermal Stimulation. In Proceedings of the 2021 CHI Conference on Human Factors in Computing Systems (CHI '21). Association for Computing Machinery, New York, NY, USA, 1–12. https://doi.org/10.1145/3411764.3445777
- [37] Jasmine Lu, Ziwei Liu, Jas Brooks, and Pedro Lopes. 2021. Chemical Haptics: Rendering Haptic Sensations via Topical Stimulants. In The 34th Annual ACM Symposium on User Interface Software and Technology (UIST '21). Association for Computing Machinery, New York, NY, USA, 239–257. https://doi.org/10.1145/ 3472749.3474747
- [38] Qiuyu Lu, Chengpeng Mao, Liyuan Wang, and Haipeng Mi. 2016. LIME: LIquid MEtal Interfaces for Non-Rigid Interaction. In Proceedings of the 29th Annual Symposium on User Interface Software and Technology (Tokyo, Japan) (UIST '16). Association for Computing Machinery, New York, NY, USA, 449–452. https://doi.org/10.1145/2984511.2984562
- [39] Qiuyu Lu, Jifei Ou, João Wilbert, André Haben, Haipeng Mi, and Hiroshi Ishii. 2019. milliMorph – Fluid-Driven Thin Film Shape-Change Materials for Interaction Design. In Proceedings of the 32nd Annual ACM Symposium on User Interface Software and Technology (UIST '19). Association for Computing Machinery, New York, NY, USA, 663–672. https://doi.org/10.1145/3332165.3347956
- [40] Qiuyu Lu, Danqing Shi, Yingqing Xu, and Haipeng Mi. 2020. MetaLife: Interactive Installation Based on Liquid Metal Deformable Interfaces. In Extended Abstracts of the 2020 CHI Conference on Human Factors in Computing Systems (Honolulu, HI, USA) (CHI EA '20). Association for Computing Machinery, New York, NY, USA, 1-4. https://doi.org/10.1145/3334480.3383134
- [41] Qiuyu Lu, Haiqing Xu, Yijie Guo, Joey Yu Wang, and Lining Yao. 2023. Fluidic Computation Kit: Towards Electronic-free Shape-changing Interfaces. In Proceedings of the 2023 CHI Conference on Human Factors in Computing Systems (CHI '23). Association for Computing Machinery, New York, NY, USA, 1–21. https://doi.org/10.1145/3544548.3580783
- [42] Danli Luo, Jianzhe Gu, Fang Qin, Guanyun Wang, and Lining Yao. 2020. E-seed: Shape-Changing Interfaces that Self Drill. In Proceedings of the 33rd Annual ACM Symposium on User Interface Software and Technology (UIST '20). Association for Computing Machinery, New York, NY, USA, 45–57. https://doi.org/10.1145/ 3379337.3415855
- [43] Kai Luo, Philipp Rothemund, George M. Whitesides, and Zhigang Suo. 2019. Soft kink valves. *Journal of the Mechanics and Physics of Solids* 131 (Oct. 2019), 230–239. https://doi.org/10.1016/j.jmps.2019.07.008
- [44] Yiyue Luo, Kui Wu, Andrew Spielberg, Michael Foshey, Daniela Rus, Tomás Palacios, and Wojciech Matusik. 2022. Digital Fabrication of Pneumatic Actuators with Integrated Sensing by Machine Knitting. In Proceedings of the 2022 CHI Conference on Human Factors in Computing Systems (CHI '22). Association for Computing Machinery, New York, NY, USA, 1–13. https://doi.org/10.1145/ 3401102.3517577
- [45] James M. Lyons. 1973. Chilling Injury in Plants. Annual Review of Plant Physiology 24, 1 (1973), 445–466. https://doi.org/10.1146/annurev.pp.24.060173.002305

- [46] Jennifer Mankoff. 2012. HCI and sustainability: a tale of two motivations. Interactions 19, 3 (May 2012), 16–19. https://doi.org/10.1145/2168931.2168937
- [47] Yogesh Kumar Meena, Krishna Seunarine, Deepak Ranjan Sahoo, Simon Robinson, Jennifer Pearson, Chi Zhang, Matt Carnie, Adam Pockett, Andrew Prescott, Suzanne K. Thomas, Harrison Ka Hin Lee, and Matt Jones. 2020. PV-Tiles: Towards Closely-Coupled Photovoltaic and Digital Materials for Useful, Beautiful and Sustainable Interactive Surfaces. In Proceedings of the 2020 CHI Conference on Human Factors in Computing Systems (CHI '20). Association for Computing Machinery, New York, NY, USA, 1–12. https://doi.org/10.1145/3313831.3376368
- [48] Haipeng Mi, Meng Wang, Qiuyu Lu, and Yingqing Xu. 2018. Tangible user interface: origins, development, and future trends. SCIENTIA SINICA Informationis 48, 4 (2018), 390–405. https://doi.org/10.1360/N112017-00227
- [49] Hila Mor, Tianyu Yu, Ken Nakagaki, Benjamin Harvey Miller, Yichen Jia, and Hiroshi Ishii. 2020. Venous Materials: Towards Interactive Fluidic Mechanisms. In Proceedings of the 2020 CHI Conference on Human Factors in Computing Systems (Honolulu, HI, USA) (CHI '20). Association for Computing Machinery, New York, NY, USA, 1–14. https://doi.org/10.1145/3313831.3376129
- [50] Takafumi Morita, Ziyuan Jiang, Kanon Aoyama, Ayato Minaminosono, Yu Kuwajima, Naoki Hosoya, Shingo Maeda, and Yasuaki Kakehi. 2023. InflatableMod: Untethered and Reconfigurable Inflatable Modules for Tabletop-Sized Pneumatic Physical Interfaces. In Proceedings of the 2023 CHI Conference on Human Factors in Computing Systems (Hamburg, Germany) (CHI '23). Association for Computing Machinery, New York, NY, USA, Article 212, 15 pages. https://doi.org/10.1145/3544548.3581353
- [51] Takafumi Morita, Yu Kuwajima, Ayato Minaminosono, Shingo Maeda, and Yasuaki Kakehi. 2022. HydroMod: Constructive Modules for Prototyping Hydraulic Physical Interfaces. In Proceedings of the 2022 CHI Conference on Human Factors in Computing Systems (CHI '22). Association for Computing Machinery, New York, NY, USA, 1–14. https://doi.org/10.1145/3491102.3502096
- [52] Kenichi Nakahara, Koya Narumi, Ryuma Niiyama, and Yoshihiro Kawahara. 2017. Electric Phase-Change Actuator with Inkjet Printed Flexible Circuit for Printable and Integrated Robot Prototyping. In 2017 IEEE International Conference on Robotics and Automation (ICRA) (Singapore, Singapore). IEEE Press, New York, NY, USA, 1856–1863. https://doi.org/10.1109/ICRA.2017.7989217
- [53] Koya Narumi, Hiroki Sato, Kenichi Nakahara, Young ah Seong, Kunihiko Morinaga, Yasuaki Kakehi, Ryuma Niiyama, and Yoshihiro Kawahara. 2020. Liquid Pouch Motors: Printable Planar Actuators Driven by Liquid-to-Gas Phase Change for Shape-Changing Interfaces. IEEE Robotics and Automation Letters 5, 3 (2020), 3915–3922. https://doi.org/10.1109/LRA.2020.2983681
- [54] PennState Department of Agricultural Sciences. 2023. Pollinator Garden Certification. https://ento.psu.edu/research/centers/pollinators/public-outreach/cert
- [55] Kazunori Ogawa, Tomohiro Ikeda, and Yuichi Kurita. 2018. Unplugged Powered Suit for Superhuman Tennis. In 2018 12th France-Japan and 10th Europe-Asia Congress on Mechatronics. IEEE Press, New York, NY, USA, 361–364. https://doi.org/10.1109/MECATRONICS.2018.8495845
- [56] Kazunori Ogawa, Chetan Thakur, Tomohiro Ikeda, Toshio Tsuji, and Yuichi Kurita. 2017. Development of a pneumatic artificial muscle driven by low pressure and its application to the unplugged powered suit. Advanced Robotics 31, 21 (Nov. 2017), 1135–1143. https://doi.org/10.1080/01691864.2017.1392345
- [57] A. G. Olabi and Mohammad Ali Abdelkareem. 2022. Renewable energy and climate change. Renewable and Sustainable Energy Reviews 158 (April 2022), 112111. https://doi.org/10.1016/j.rser.2022.112111
- [58] Jifei Ou, Mélina Skouras, Nikolaos Vlavianos, Felix Heibeck, Chin-Yi Cheng, Jannik Peters, and Hiroshi Ishii. 2016. aeroMorph - Heat-sealing Inflatable Shapechange Materials for Interaction Design. In Proceedings of the 29th Annual Symposium on User Interface Software and Technology (UIST '16). Association for Computing Machinery, New York, NY, USA, 121–132. https://doi.org/10.1145/ 2984511.2984520
- [59] Judith E. Pasek. 1988. 30. Influence of wind and windbreaks on local dispersal of insects. Agriculture, Ecosystems & Environment 22-23 (Aug. 1988), 539–554. https://doi.org/10.1016/0167-8809(88)90044-8
- [60] Marissa V. Ponder, Gordon W. Frankie, Rachel Elkins, Kate Frey, Rollin Coville, Mary Schindler, Sara Leon Guerrero, Jaime C. Pawelek, and Carolyn Shaffer. 2013. How to Attract and Maintain Pollinators in Your Garden. n/a n/a, n/a (Oct. 2013), 13. https://doi.org/10.3733/ucanr.8498
- [61] Daniel J. Preston, Haihui Joy Jiang, Vanessa Sanchez, Philipp Rothemund, Jeff Rawson, Markus P. Nemitz, Won-Kyu Lee, Zhigang Suo, Conor J. Walsh, and George M. Whitesides. 2019. A soft ring oscillator. Science Robotics 4, 31 (June 2019), eaaw5496. https://doi.org/10.1126/scirobotics.aaw5496
- [62] Daniel J. Preston, Philipp Rothemund, Haihui Joy Jiang, Markus P. Nemitz, Jeff Rawson, Zhigang Suo, and George M. Whitesides. 2019. Digital logic for soft devices. *Proceedings of the National Academy of Sciences* 116, 16 (April 2019), 7750–7759. https://doi.org/10.1073/pnas.1820672116
- [63] Drew Swainston published. 2023. When to fertilize seedlings to encourage strong and healthy growth. https://www.homesandgardens.com/gardens/whento-fertilize-seedlings
- [64] Atika Qazi, Fayaz Hussain, Nasrudin ABD. Rahim, Glenn Hardaker, Daniyal Alghazzawi, Khaled Shaban, and Khalid Haruna. 2019. Towards Sustainable

- Energy: A Systematic Review of Renewable Energy Sources, Technologies, and Public Opinions. *IEEE Access* 7 (2019), 63837–63851. https://doi.org/10.1109/ACCESS.2019.2906402
- [65] Anoop Rajappan, Barclay Jumet, and Daniel J. Preston. 2021. Pneumatic soft robots take a step toward autonomy. *Science Robotics* 6, 51 (Feb. 2021), eabg6994. https://doi.org/10.1126/scirobotics.abg6994
- [66] Anoop Rajappan, Barclay Jumet, Rachel A. Shveda, Colter J. Decker, Zhen Liu, Te Faye Yap, Vanessa Sanchez, and Daniel J. Preston. 2022. Logic-enabled textiles. Proceedings of the National Academy of Sciences 119, 35 (Aug. 2022), e2202118119. https://doi.org/10.1073/pnas.2202118119
- [67] Terry S. Reynolds. 1983. Stronger Than a Hundred Men: A History of the Vertical Water Wheel. JHU Press, n/a. Google-Books-ID: aZ0runvrq0AC.
- [68] Philipp Rothemund, Alar Ainla, Lee Belding, Daniel J. Preston, Sarah Kurihara, Zhigang Suo, and George M. Whitesides. 2018. A soft, bistable valve for autonomous control of soft actuators. Science Robotics 3, 16 (March 2018), eaar7986. https://doi.org/10.1126/scirobotics.aar7986
- [69] Vanessa Sanchez, Christopher J. Payne, Daniel J. Preston, Jonathan T. Alvarez, James C. Weaver, Asli T. Atalay, Mustafa Boyvat, Daniel M. Vogt, Robert J. Wood, George M. Whitesides, and Conor J. Walsh. 2020. Smart Thermally Actuating Textiles. Advanced Materials Technologies 5, 8 (2020), 2000383. https://doi.org/10.1002/admt.202000383 arXiv:https://onlinelibrary.wiley.com/doi/pdf/10.1002/admt.202000383
- [70] Harpreet Sareen, Udayan Umapathi, Patrick Shin, Yasuaki Kakehi, Jifei Ou, Hiroshi Ishii, and Pattie Maes. 2017. Printflatables: Printing Human-Scale, Functional and Dynamic Inflatable Objects. In Proceedings of the 2017 CHI Conference on Human Factors in Computing Systems (CHI '17). Association for Computing Machinery, New York, NY, USA, 3669–3680. https://doi.org/10.1145/3025453. 3025898
- [71] Valkyrie Savage, Carlos Tejada, Mengyu Zhong, Raf Ramakers, Daniel Ashbrook, and Hyunyoung Kim. 2022. AirLogic: Embedding Pneumatic Computation and I/O in 3D Models to Fabricate Electronics-Free Interactive Objects. In Proceedings of the 35th Annual ACM Symposium on User Interface Software and Technology (UIST '22). Association for Computing Machinery, New York, NY, USA, 1–12. https://doi.org/10.1145/3526113.3545642
- [72] Jeroen ter Schiphorst, Janire Saez, Dermot Diamond, Fernando Benito-Lopez, and Albertus P. H. J. Schenning. 2018. Light-responsive polymers for microfluidic applications. Lab on a Chip 18, 5 (Feb. 2018), 699–709. https://doi.org/10.1039/ C7LC01297G
- [73] Hu Shi, Zhaoying Liu, and Xuesong Mei. 2020. Overview of Human Walking Induced Energy Harvesting Technologies and Its Possibility for Walking Robotics. Energies 13, 1 (Jan. 2020), 86. https://doi.org/10.3390/en13010086
- [74] Rachel A. Shveda, Anoop Rajappan, Te Faye Yap, Zhen Liu, Marquise D. Bell, Barclay Jumet, Vanessa Sanchez, and Daniel J. Preston. 2022. A wearable textilebased pneumatic energy harvesting system for assistive robotics. *Science Advances* 8, 34 (Aug. 2022), eabo2418. https://doi.org/10.1126/sciadv.abo2418
- [75] Katherine W Song, Aditi Maheshwari, Eric M Gallo, Andreea Danielescu, and Eric Paulos. 2022. Towards Decomposable Interactive Systems: Design of a Backyard-Degradable Wireless Heating Interface. In Proceedings of the 2022 CHI Conference on Human Factors in Computing Systems (CHI '22). Association for Computing Machinery, New York, NY, USA, 1–12. https://doi.org/10.1145/3491102.3502007
- [76] Saya Suzunaga, Yuichi Itoh, Yuki Inoue, Kazuyuki Fujita, and Takao Onoye. 2020. TuVe: A Shape-changeable Display using Fluids in a Tube. In Proceedings of the International Conference on Advanced Visual Interfaces (AVI '20). Association for Computing Machinery, New York, NY, USA, 1–9. https://doi.org/10.1145/ 3399715.3399874
- [77] Matteo Taffetani, Xin Jiang, Douglas P. Holmes, and Dominic Vella. 2018. Static bistability of spherical caps. Proceedings of the Royal Society A: Mathematical, Physical and Engineering Sciences 474, 2213 (May 2018), 20170910. https://doi. org/10.1098/rspa.2017.0910
- [78] Shuai Tang, Jiao Li, Runguo Wang, Jichuan Zhang, Yonglai Lu, Guo-Hua Hu, Zhao Wang, and Liqun Zhang. 2022. Current trends in bio-based elastomer materials. SusMat 2, 1 (2022), 2–33. https://doi.org/10.1002/sus2.45
- [79] Carlos E. Tejada, Raf Ramakers, Sebastian Boring, and Daniel Ashbrook. 2020. AirTouch: 3D-printed Touch-Sensitive Objects Using Pneumatic Sensing. In Proceedings of the 2020 CHI Conference on Human Factors in Computing Systems (CHI '20). Association for Computing Machinery, New York, NY, USA, 1–10. https://doi.org/10.1145/3313831.3376136
- [80] Shan-Yuan Teng, Tzu-Sheng Kuo, Chi Wang, Chi-huan Chiang, Da-Yuan Huang, Liwei Chan, and Bing-Yu Chen. 2018. PuPoP: Pop-up Prop on Palm for Virtual Reality. In Proceedings of the 31st Annual ACM Symposium on User Interface Software and Technology (UIST '18). Association for Computing Machinery, New York, NY, USA, 5–17. https://doi.org/10.1145/3242587.3242628
- [81] Shan-Yuan Teng, Cheng-Lung Lin, Chi-huan Chiang, Tzu-Sheng Kuo, Liwei Chan, Da-Yuan Huang, and Bing-Yu Chen. 2019. Tile-PoP: Tile-type Pop-up Prop for Virtual Reality. In Proceedings of the 32nd Annual ACM Symposium on User Interface Software and Technology (UIST '19). Association for Computing Machinery, New York, NY, USA, 639–649. https://doi.org/10.1145/3332165.3347958

- [82] Shan-Yuan Teng, K. D. Wu, Jacqueline Chen, and Pedro Lopes. 2022. Prolonging VR Haptic Experiences by Harvesting Kinetic Energy from the User. In Proceedings of the 35th Annual ACM Symposium on User Interface Software and Technology (UIST '22). Association for Computing Machinery, New York, NY, USA, 1–18. https://doi.org/10.1145/3526113.3545635
- [83] Michael Uebelacker and Dirk W. Lachenmeier. 2011. Quantitative Determination of Acetaldehyde in Foods Using Automated Digestion with Simulated Gastric Fluid Followed by Headspace Gas Chromatography. *Journal of Automated Methods and Management in Chemistry* 2011 (2011), 907317. https://doi.org/10.1155/2011/907317
- [84] Eldy S. Lazaro Vasquez and Katia Vega. 2019. From plastic to biomaterials: prototyping DIY electronics with mycelium. In Adjunct Proceedings of the 2019 ACM International Joint Conference on Pervasive and Ubiquitous Computing and Proceedings of the 2019 ACM International Symposium on Wearable Computers (UbiComp/ISWC '19 Adjunct). Association for Computing Machinery, New York, NY, USA, 308–311. https://doi.org/10.1145/3341162.3343808
- [85] Nicolas Villar and Steve Hodges. 2010. The peppermill: a human-powered user interface device. In Proceedings of the fourth international conference on Tangible, embedded, and embodied interaction (TEI '10). Association for Computing Machinery, New York, NY, USA, 29–32. https://doi.org/10.1145/1709886.1709927
- [86] Marynel Vázquez, Eric Brockmeyer, Ruta Desai, Chris Harrison, and Scott E. Hudson. 2015. 3D Printing Pneumatic Device Controls with Variable Activation Force Capabilities. In Proceedings of the 33rd Annual ACM Conference on Human Factors in Computing Systems (CHI '15). Association for Computing Machinery, New York, NY, USA, 1295–1304. https://doi.org/10.1145/2702123.2702569
- [87] A. M. Waddell, J. Punch, J. Stafford, and N. Jeffers. 2015. On the hydrodynamic characterization of a passive Shape Memory Alloy valve. *Applied Thermal Engi*neering 75 (Jan. 2015), 731–737. https://doi.org/10.1016/j.applthermaleng.2014. 09.073
- [88] Ludwig Wilhelm Wall, Alec Jacobson, Daniel Vogel, and Oliver Schneider. 2021. Scrappy: Using Scrap Material as Infill to Make Fabrication More Sustainable. In Proceedings of the 2021 CHI Conference on Human Factors in Computing Systems (CHI '21). Association for Computing Machinery, New York, NY, USA, 1–12. https://doi.org/10.1145/3411764.3445187
- [89] Penelope Webb, Valentina Sumini, Amos Golan, and Hiroshi Ishii. 2019. Auto-Inflatables: Chemical Inflation for Pop-Up Fabrication. In Extended Abstracts of the 2019 CHI Conference on Human Factors in Computing Systems (CHI EA '19). Association for Computing Machinery, New York, NY, USA, 1-6. https: //doi.org/10.1145/3290607.3312860
- [90] Michael Wehner, Ryan L. Truby, Daniel J. Fitzgerald, Bobak Mosadegh, George M. Whitesides, Jennifer A. Lewis, and Robert J. Wood. 2016. An integrated design and fabrication strategy for entirely soft, autonomous robots. *Nature* 536, 7617 (Aug. 2016), 451–455. https://doi.org/10.1038/nature19100
- [91] Chen Xu, Yu Song, Mengdi Han, and Haixia Zhang. 2021. Portable and wearable self-powered systems based on emerging energy harvesting technology. *Microsystems & Nanoengineering* 7, 1 (March 2021), 1–14. https://doi.org/10.1038/s41378-021-00248-z
- [92] Junichi Yamaoka, Ryuma Niiyama, and Yasuaki Kakehi. 2017. BlowFab: Rapid Prototyping for Rigid and Reusable Objects using Inflation of Laser-cut Surfaces. In Proceedings of the 30th Annual ACM Symposium on User Interface Software and Technology (UIST '17). Association for Computing Machinery, New York, NY, USA, 461–469. https://doi.org/10.1145/3126594.3126624
- [93] Junichi Yamaoka, Kazunori Nozawa, Shion Asada, Ryuma Niiyama, Yoshihiro Kawahara, and Yasuaki Kakehi. 2018. AccordionFab: Fabricating Inflatable 3D

- Objects by Laser Cutting and Welding Multi-Layered Sheets. In *Adjunct Proceedings of the 31st Annual ACM Symposium on User Interface Software and Technology (UIST '18 Adjunct)*. Association for Computing Machinery, New York, NY, USA, 160–162. https://doi.org/10.1145/3266037.3271636
- [94] Lining Yao, Ryuma Niiyama, Jifei Ou, Sean Follmer, Clark Della Silva, and Hiroshi Ishii. 2013. PneUI: pneumatically actuated soft composite materials for shape changing interfaces. In Proceedings of the 26th annual ACM symposium on User interface software and technology (UIST '13). Association for Computing Machinery, New York, NY, USA, 13–22. https://doi.org/10.1145/2501988.2502037
- [95] Tianyu Yu, Weiye Xu, Haiqing Xu, Guanhong Liu, Chang Liu, Guanyun Wang, and Haipeng Mi. 2023. Thermotion: Design and Fabrication of Thermofluidic Composites for Animation Effects on Object Surfaces. In Proceedings of the 2023 CHI Conference on Human Factors in Computing Systems (Hamburg, Germany) (CHI '23). Association for Computing Machinery, New York, NY, USA, Article 425, 19 pages. https://doi.org/10.1145/3544548.3580743

A SUPPLEMENTARY MATERIAL INFORMATION

- 1-Readme
- 2-Design tool
- 3-Pump
 - Thermal Pump
 - * Material List and Assembly Instruction
 - * All model files
 - Moisture Pump
 - * Material List and Assembly Instruction
 - * All model files
 - Kinetic Pump
 - * Material List and Assembly Instruction
 - * All model files
- 4-Valve
 - Bursting Valve
 - * Material List and Assembly Instruction
 - * All model files
 - Moisture Valve
 - * Material List and Assembly Instruction
 - * All model files
 - NC Thermal Valve
 - * Material List and Assembly Instruction
 - * All model files
 - NO Thermal Valve
 - * Material List and Assembly Instruction
 - * All model files